LIST OF PUBLICATIONS

AS FIRST AUTHOR

1 **Venkatesan V**, Christopher AC, Rhiel M, Kumar M, Azhagiri K, Babu P *et al.* Editing the core region in HPFH deletions alters fetal and adult globin expression for treatment of β-hemoglobinopathies. *Mol Ther - Nucleic Acids* 2023; **32**: 671–688.

2 **Venkatesan V**, Christopher AC, Karuppusamy K V., Babu P, Alagiri MKK, Thangavel S. CRISPR/Cas9 Gene Editing of Hematopoietic Stem and Progenitor Cells for Gene Therapy Applications. *JoVE (Journal Vis Exp* 2022; **2022**: e64064.

3 **Christopher AC**, **Venkatesan V**, Karuppusamy K V, Srinivasan S, Babu P, Azhagiri MKK *et al.* Preferential expansion of human CD34+CD133+CD90+ hematopoietic stem cells enhances gene-modified cell frequency for gene therapy. *Hum Gene Ther* 2021; : 1–33.

4 **Venkatesan V**, Srinivasan S, Babu P, Thangavel S. Manipulation of Developmental Gamma-Globin Gene Expression: an Approach for Healing Hemoglobinopathies. *Mol Cell Biol* 2020; **41**: 1–18.

AS CO-AUTHOR

1 Lohchania B, Christopher AC, Arjunan P, Mahalingam G, Kathirvelu D, Prasannan A *et al.* Diosgenin enhances liposome-enabled nucleic acid delivery and CRISPR/Cas9-mediated gene editing by modulating endocytic pathways. *Front Bioeng Biotechnol* 2023; **10**: 1–8.

2 Rapaka H, Manturthi S, Arjunan P, **Venkatesan V**, Thangavel S, Marepally S *et al.* Influence of Hydrophobicity in the Hydrophilic Region of Cationic Lipids on Enhancing Nucleic Acid Delivery and Gene Editing. *ACS Appl Bio Mater* 2022; **5**: 1489–1500.

3 Prasad K, Devaraju N, George A, Ravi NS, Mahalingam G, Rajendiran V *et al.* Precise modelling and correction of a spectrum of β-thalassemic mutations in human erythroid cells by base editors. *bioRxiv* 2022; : 2022.06.01.494256.

4 Karuppusamy K V., Demosthenes JP, **Venkatesan V**, Christopher AC, Babu P, Azhagiri MK *et al.* The CCR5 Gene Edited CD34+CD90+ Hematopoietic Stem Cell Population Serves as an Optimal Graft Source for HIV Gene Therapy. *Front Immunol* 2022; **13**: 792684.

5 Bagchi A, Devaraju N, Chambayil K, Rajendiran V, **Venkatesan V**, Sayed N *et al.* Erythroid lineage-specific lentiviral RNAi vectors suitable for molecular functional studies and therapeutic applications. *Sci Rep* 2022; **12**: 1–13.

6 Bagchi A, Nath A, Thamodaran V, Ijee S, Palani D, Rajendiran V *et al.* Direct Generation of Immortalized Erythroid Progenitor Cell Lines from Peripheral Blood Mononuclear Cells. *Cells* 2021; **10**: 1–18.

7 Azhagiri MKK, Babu P, **Venkatesan V**, Thangavel S. Homology - directed gene - editing approaches for hematopoietic stem and progenitor cell gene therapy. *Stem Cell Res Ther* 2021; : 1–12.

Molecular Therapy
Nucleic Acids
Original Article

Editing the core region in HPFH deletions alters fetal and adult globin expression for treatment of β-hemoglobinopathies

Vigneshwaran Venkatesan,[1,2] Abisha Crystal Christopher,[1] Manuel Rhiel,[3,4] Manoj Kumar K. Azhagiri,[1,2] Prathibha Babu,[1,2] Kaivalya Walavalkar,[5] Bharath Saravanan,[5] Geoffroy Andrieux,[6,7] Sumathi Rangaraj,[1] Saranya Srinivasan,[1] Karthik V. Karuppusamy,[1,2] Annlin Jacob,[1] Abhirup Bagchi,[1] Aswin Anand Pai,[8] Yukio Nakamura,[9] Ryo Kurita,[9] Poonkuzhali Balasubramanian,[8] Rekha Pai,[10] Srujan Kumar Marepally,[1] Kumarasamypet Murugesan Mohankumar,[1] Shaji R. Velayudhan,[1,8] Melanie Boerries,[6,7] Dimple Notani,[5] Toni Cathomen,[3,4] Alok Srivastava,[1,8] and Saravanabhavan Thangavel[1]

[1]Centre for Stem Cell Research (CSCR), A Unit of InStem Bengaluru, Christian Medical College Campus, Vellore, Tamil Nadu 632002, India; [2]Manipal Academy of Higher Education, Manipal 576104, Karnataka, India; [3]Institute for Transfusion Medicine and Gene Therapy, Medical Center – University of Freiburg, 79106 Freiburg, Germany; [4]Center for Chronic Immunodeficiency, Medical Faculty, University of Freiburg, 79106 Freiburg, Germany; [5]National Centre for Biological Sciences, Tata Institute of Fundamental Research, Bangalore, Karnataka 560065, India; [6]Institute of Medical Bioinformatics and Systems Medicine, Faculty of Medicine & Medical Center - University of Freiburg, 79106 Freiburg, Germany; [7]German Cancer Consortium (DKTK), Partner Site Freiburg and German Cancer Research Center (DKFZ), 69120 Heidelberg, Germany; [8]Department of Hematology, Christian Medical College, Vellore, Tamil Nadu 632004, India; [9]Cell Engineering Division, RIKEN BioResource Research Center, Ibaraki 3050074, Japan; [10]Department of Pathology, Christian Medical College, Vellore, Tamil Nadu 632004, India

Reactivation of fetal hemoglobin (HbF) is a commonly adapted strategy to ameliorate β-hemoglobinopathies. However, the continued production of defective adult hemoglobin (HbA) limits HbF tetramer production affecting the therapeutic benefits. Here, we evaluated deletional hereditary persistence of fetal hemoglobin (HPFH) mutations and identified an 11-kb sequence, encompassing putative repressor region (PRR) to β-globin exon-1 (βE1), as the core deletion that ablates HbA and exhibits superior HbF production compared with HPFH or other well-established targets. PRR-βE1-edited hematopoietic stem and progenitor cells (HSPCs) retained their genome integrity and their engraftment potential to repopulate for long-term hematopoiesis in immunocompromised mice producing HbF positive cells *in vivo*. Furthermore, PRR-βE1 gene editing is feasible without *ex vivo* HSPC culture. Importantly, the editing induced therapeutically significant levels of HbF to reverse the phenotypes of both sickle cell disease and β-thalassemia major. These findings imply that PRR-βE1 gene editing of patient HSPCs could lead to improved therapeutic outcomes for β-hemoglobinopathy gene therapy.

INTRODUCTION

β-Hemoglobinopathies—β-thalassemia and sickle cell disease (SCD)—are highly prevalent inherited globin chain disorders that are autosomal recessive. They account for 3.4% of mortalities in children younger than 5 years.[1,2] β-thalassemia is caused by more than 300 different mutations in the β-globin gene or its flanking nucleotides; these mutations impair the synthesis of the β-globin chain, affecting the tightly coordinated equilibrium of adult hemoglobin ($HbA/\alpha_2\beta_2$) chains.[3] The excess free α-globin precipitates in erythroblasts and induces apoptosis, resulting in ineffective erythropoiesis.[4] SCD is caused by the E6V (rs334) missense mutation in the β-globin gene. This mutation causes polymerization of deoxygenated sickle hemoglobin (HbS) tetramers, which severely reduces the circulating lifespan of red blood cells (RBCs) and eventually causes vascular damage and progressive multiorgan damage.[5]

Morbidity in β-thalassemia and SCD patients is inversely correlated with the levels of fetal hemoglobin (HbF) in adulthood.[6,7] Expression of γ-globin, the fetal β-like globin component of HbF, improves the globin chain equilibrium and thus prevents apoptosis of erythroid cells in β-thalassemia. Similarly, in SCD, γ-globin competes with the sickle β-globin chains (βs) to form HbF tetramers ($\alpha_2\gamma_2$), thereby reducing the production of sickle RBCs. Hence, several studies are focused on identifying and manipulating genetic factors involved in HbF regulation.[8–10] Two recent clinical studies involving short hairpin RNA (shRNA)-mediated erythroid-specific downregulation of BCL11A and gene-editing-mediated disruption of its erythroid-specific enhancer have demonstrated reactivated HbF levels sufficient to reach transfusion independence.[11,12] However, up to 50% of hemoglobin remained as HbS in the SCD patients; thus, strategies that reduce or eliminate defective β-globin production are worth further exploration.

Received 17 December 2022; accepted 24 April 2023;
https://doi.org/10.1016/j.omtn.2023.04.024.

Correspondence: Saravanabhavan Thangavel, Centre for Stem Cell Research (CSCR), A Unit of InStem Bengaluru, Christian Medical College Campus, Vellore, Tamil Nadu 632002, India.
E-mail: sthangavel@cmcvellore.ac.in

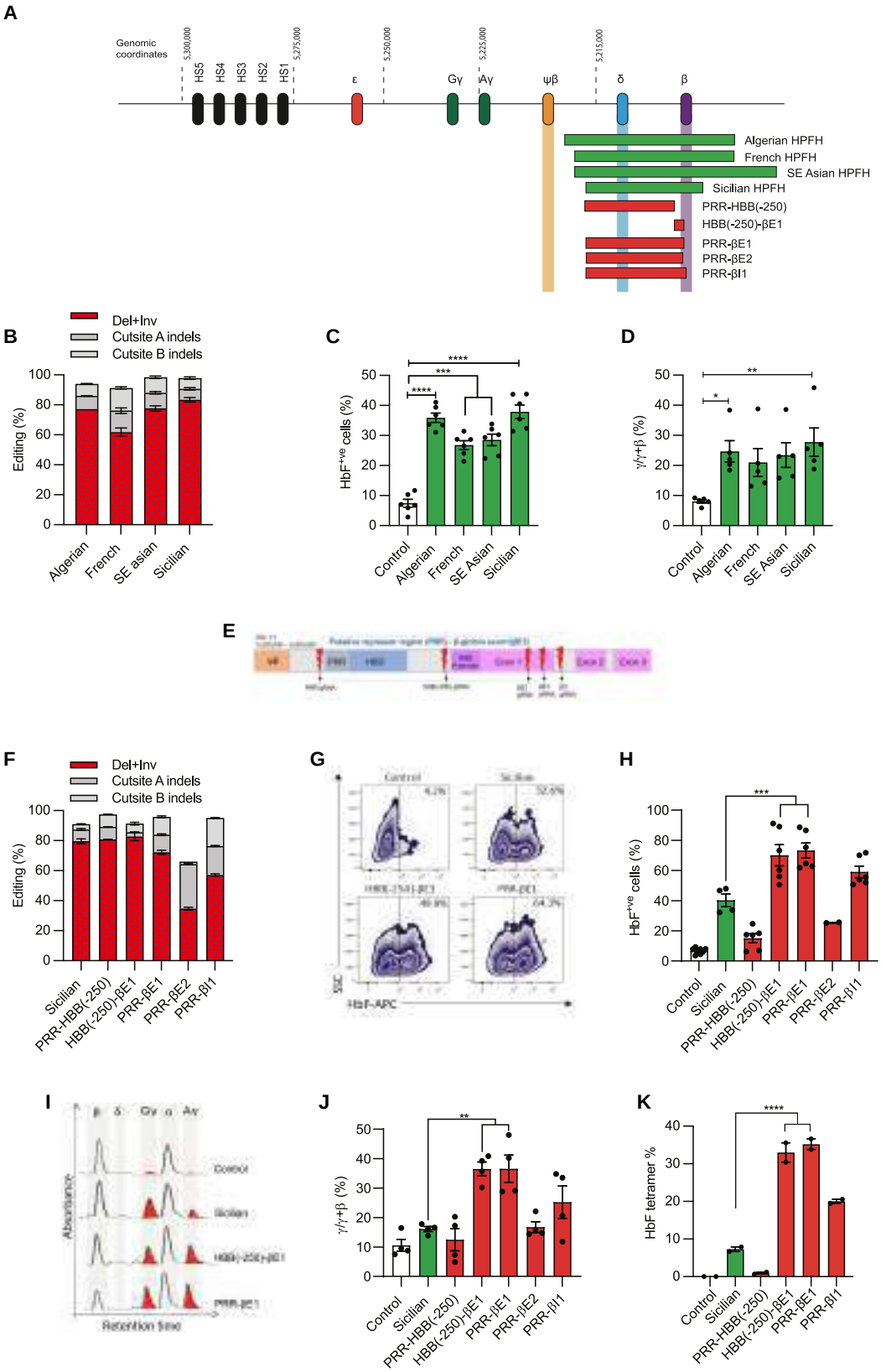

(legend on next page)

Mutations causing hereditary persistence of fetal hemoglobin (HPFH) are documented to produce varying levels of HbF in healthy individuals without any deleterious effects.[13] Importantly, the HPFH mutations are beneficial in alleviating disease severity when co-inherited with β-hemoglobinopathies.[14] Among the genetic variants that induce HbF expression, deletional HPFH mutations produce higher levels of HbF and are highly prevalent.[15] β-Globin production is ablated in HPFH deletions, distinguishing them from other HbF reactivating mutations. HPFH deletions range in size from 12.9 to 84.9 kb, encompassing *HBG1*, *HBBP1*, *HBD,* and *HBB* genes in the β-globin cluster, and result in pancellular HbF production.[16] The introduction of HPFH deletions in adult hematopoietic stem and progenitor cells (HSPCs) results in activation of γ-globin with subsequent amelioration of the sickle phenotype.[17,18] However, much is still unknown, such as the minimal genomic deletion required for therapeutically relevant γ-globin activation, genome integrity, engraftment, and repopulation potential of HSPCs harboring such genomic deletions and their efficacy in reversing the disease phenotype. In a very recent study, Topfer et al. showed that the deletion of the proximal promoter of HBB, excised in HPFH and δβ-thalassemia deletions, is sufficient for γ-globin activation.[19]

To investigate the translational potential of HSPCs with deletional HPFH mutations, we used CRISPR-Cas9 to screen multiple HPFH deletions and identified an 11-kb core-regulatory region from putative repressor region (PRR) to β-globin exon-1 (βE1) (PRR-βE1). Gene editing of PRR-βE1 repressed the β-globin and activated γ-globin to levels greater than known candidates targeting the BCL11A enhancer and HBG promoter region, reversing the SCD and β-thalassemia phenotypes. We also demonstrated long-term hematopoiesis of the edited HSPCs and achieved efficient editing without cytokine pre-stimulation and genotoxicity.

RESULTS

Genomic deletion encompassing PRR to βE1 is sufficient to reproduce deletional HPFH phenotype

To identify an HPFH deletion suitable for therapeutic gene editing, we introduced deletional HPFH mutations of <30 kb in size, mirroring the Algerian[20] (24 kb), French[20] (20 kb), Southeast (SE) Asian[21] (27 kb), and Sicilian[22] (12.9 kb) genotypes, by CRISPR-Cas9 dual guide RNA (gRNA) gene editing in the HUDEP-2 cell line (Figure 1A). The 7.2-kb Corfu deletion, which is now considered as δβ-thalassemia and requires homozygous deletion to activate therapeutic HbF levels,[17,23] was excluded from our screening. The efficiency of gene editing was assessed using droplet digital polymerase chain reaction (ddPCR) and Sanger sequencing in conjunction with Inference of CRISPR Edits (ICE) analysis.

All candidates exhibited >60% editing efficiency (Figure 1B). Erythroid differentiation of gene-edited HUDEP-2 cells showed an increased percentage of HbF^{+ve} cells (Figure 1C), γ-globin messenger RNA (mRNA) (Figure S1A), activation of γ-globin chains (Figure 1D), and decreased production of β-globin chains (Figure S1B) in all HPFH deletions. Sicilian HPFH produced a marginally higher level of γ-globin chains than the other targets, and is the central region among the HPFH deletions.

To decipher the HbF regulatory region in the Sicilian HPFH deletion, we excised different regions spanning the deletion, such as PRR to the upstream region of β-globin promoter (PRR-HBB(-250)), promoter to exon-1 (HBB(-250)-βE1), PRR to exon-1 (PRR-βE1), PRR to intron-1 (PRR-βI1), and PRR to exon-1 CD27 (PRR-βE2) of the β-globin gene (Figures 1A, 1E, and 1F). Among these candidates, HBB(-250)-βE1 and PRR-βE1 showed a 1.8-fold higher percentage of HbF^{+ve} cells than the Sicilian HPFH (Figures 1G and 1H). Both candidates showed a substantial increase in the γ-globin activation (Figures 1I, 1J, and S1C) with decreased β-globin levels (Figure S1D). Sicilian HPFH favored Gγ activation, whereas the PRR-βE1 and HBB(-250)-βE1-edited cells displayed equivalent activation of both Aγ and Gγ chains (Figure S1E). Variant high-performance liquid chromatography (HPLC) analysis confirmed the functional HbF tetramer in both these samples, and they had a greater than 4-fold higher proportion of HbF tetramers than the Sicilian HPFH (Figure 1K).

To understand why Sicilian HPFH reactivates less γ-globin levels than HBB(-250)-βE1 and PRR-βE1, which are the regions within Sicilian HPFH, we single-cell sorted Sicilian HPFH edited HUDEP-2

Figure 1. Genomic deletion encompassing PRR to βE1 is sufficient to reproduce deletional HPFH phenotype

(A) Diagrammatic representation of β-globin cluster and the break points of naturally occurring HPFH deletions (green). These deletions are introduced in the experiments shown in (B)–(D). Break points of deletions (red) introduced in the experiment shown in (F)–(K). All these deletions were generated in HUDEP-2 cell lines by CRISPR-Cas9 dual gRNA approach. (B) Percentage of gene editing in HUDEP-2 cell lines, gene edited for HPFH deletions. Type of HPFH deletions are indicated at the x axis. Indels (cut site A and cut site B) measured by Sanger sequencing and ICE analysis. Deletion + Inversion (Del+Inv) (red checker box) quantified by ddPCR. n = 2. (C) Percentage of HbF^{+ve} cells upon introducing HPFH deletions indicated on the x axis. The edited cells were differentiated into erythroblasts and analyzed for HbF by flow cytometry. n = 6. (D) γ-Globin chain synthesis as measured by γ/γ+β ratio in the HUDEP-2 erythroblasts as measured by HPLC chain analysis. n = 5. (E) Magnified image of β-globin locus showing the binding sites of the key gRNA employed in this study to create various deletions mentioned in (F)–(K). (F) Percentage of gene editing in HUDEP-2 cell lines gene edited for various deletions as indicated in the x axis. Indels (cut site A and cut site B) measured by Sanger sequencing and ICE analysis. Deletion + Inversion (Del+Inv) (red checker box) quantified by ddPCR. n = 2. (G) Representative flow cytometry plot of HbF^{+ve} cells. HUDEP-2 cell lines gene edited for Sicilian HPFH deletion and deletion of its encompassing region in the β-globin cluster, were differentiated into erythroblasts and analyzed for HbF^{+ve} cells. Inset shows percentage of HbF^{+ve} cells. (H) Percentage of HbF^{+ve} cells upon introducing deletions in the region encompassing Sicilian HPFH. n = 4. (I) Representative globin chain HPLC chromatograms. (J) γ-Globin chain synthesis as measured by γ/γ+β ratio in the HUDEP-2 cell lines as measured by HPLC chain analysis. n = 4. (K) Percentage of HbF tetramer in erythroid differentiated HUDEP-2 cells gene edited for introducing deletions in the region encompassing Sicilian HPFH as measured by variant HPLC analysis. n = 2. Error bars represent mean ± SEM, *p ≤ 0.05, **p ≤ 0.01, ***p ≤ 0.001, ****p ≤ 0.0001 (one-way ANOVA followed by Dunnett's multiple comparisons test).

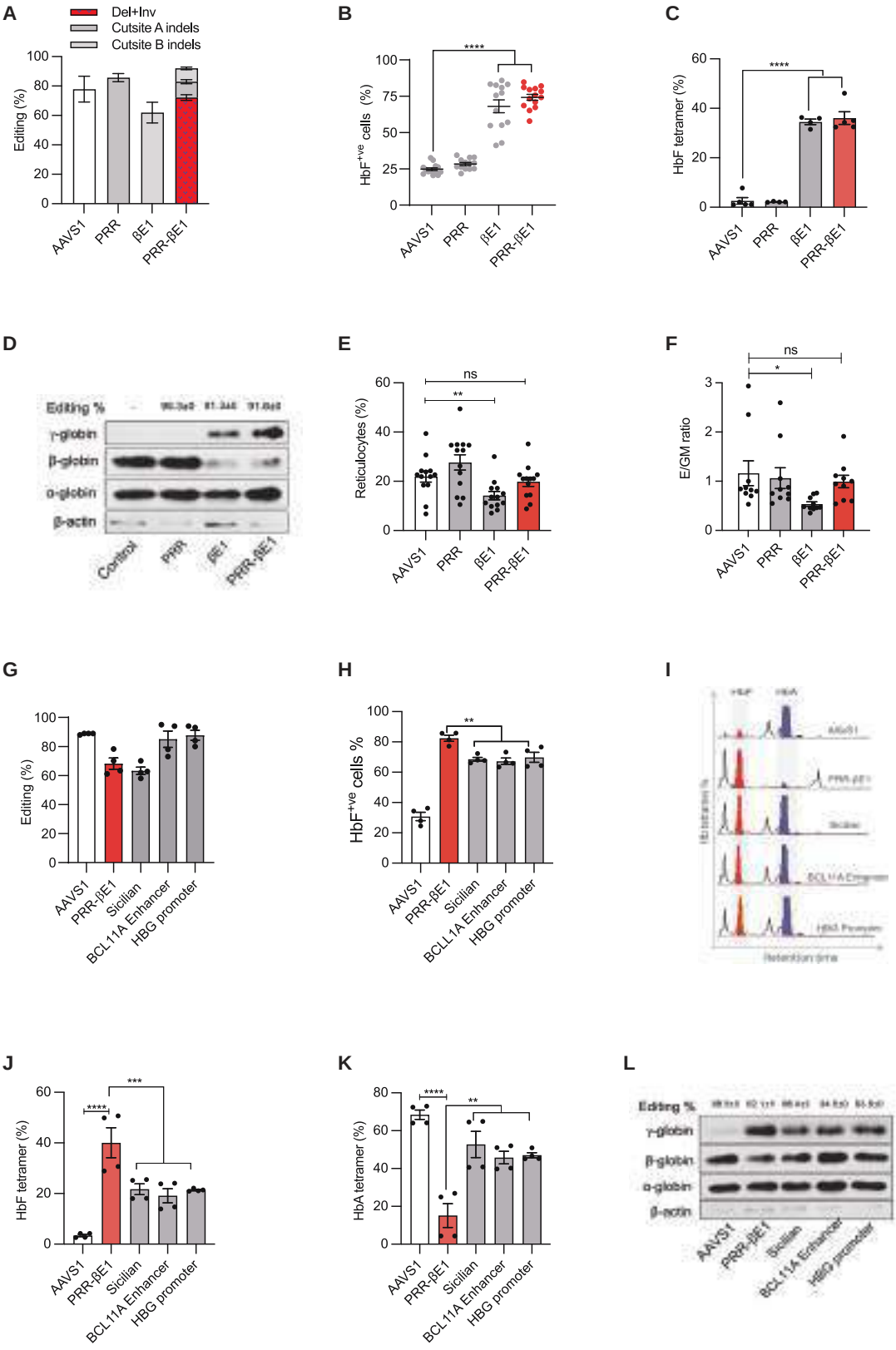

(legend on next page)

cells and generated clonal lines with inversion or deletions. Interestingly, HPLC analysis revealed intact β-globin expression and indicated no substantial increase of γ-globin in inversion clones. Contrastingly, clones with deletions exhibited decreased β-globin chains and activation of γ-globin. Similar trend was also observed with French HPFH (Figures S1F and S1G). This shows that inversion results in alterations of β-globin cluster orientation without impacting the γ-globin gene expression. Also, this observation explains why the β-globin levels are intact in Sicilian HPFH despite high gene editing efficiency. On the contrary, the inversion events on HBB(-250)-βE1 and PRR-βE1 editing disrupts the β-globin exonic regions and such events are reported to block the β-globin expression.[18]

The PRR-βE1 region is excised in all the deletional HPFH mutations (Figure S2). The sequence spanning PRR is completely or partially intact in δβ-thalassemia and β-thalassemia deletions, suggesting it as a region that distinguishes HPFH and thalassemia phenotypes. Whereas, HBB(-250)-βE1 deletion resembles the British black and Croatian β-thalassemia genotypes[24,25] and was also reported recently as a target for HbF reactivation.[19] Therefore PRR-βE1 was considered for further studies. The ddPCR-mediated quantification of PRR-βE1 gene-editing analysis (Figures S3A and S3B) was further confirmed by gap PCR analysis in the sorted single-cell clones (Figures S3C and S3D).

Robust γ-globin induction and β-globin silencing in the erythroblasts differentiated from PRR-βE1-edited HSPCs

To investigate the effect of PRR-βE1 editing in therapeutically relevant cells, granulocyte colony-stimulating factor (G-CSF)-mobilized HSPCs from five healthy donors were electroporated with Cas9 ribonucleoproteins (RNPs) targeting cut site A - PRR and cut site B - βE1 sites individually and in combination. The total gene-editing efficiency in PRR-βE1 was 92% ± 4%, among which PRR-βE1 deletion and inversion (del+inv) comprised 72.1% ± 2% (Figure 2A). The viability of PRR-βE1-edited HSPCs remained similar to that of *AAVS1*-edited cells (Figure S4A). Upon differentiation of HSPCs into erythroblasts using a three-phase *in vitro* erythroid differentiation protocol, a significant increase in the percentage of HbF^{+ve} cells was observed in PRR-βE1 (74.2% ± 3%) and βE1-edited cells (68.0% ± 3%) relative to the *AAVS1* control (24.7% ± 3%) (Figure 2B). Variant HPLC analysis showed up to 13-fold higher levels of HbF tetramers and up to 5-fold reduced levels of HbA tetramers upon βE1 and PRR-βE1 editing (Figures 2C and S4B). Consistent with all aforementioned analyses, RT-PCR analysis (Figure S4C) and western blot confirmed the increased γ-globin and decreased β-globin expression (Figures 2D and S4D), quantitatively confirming the absolute levels of γ-globin produced on PRR-βE1 gene editing.

The frequency of gene editing in HSPCs and erythroblasts derived from gene-edited HSPCs did not differ significantly (Figure S4E). The erythroid maturation analysis using CD235a and Hoechst, showed that PRR-βE1-edited cells had comparable levels of reticulocytes with the control, whereas the percentage of reticulocytes was significantly lower in βE1-edited cells (Figure 2E). A similar trend was observed with a different set of erythroid markers $CD235a^{+}$/$CD71^{-}$ (Figure S4F).

Similarly, in PRR-βE1 editing, erythroid colony-forming potential as assessed by the ratio of erythroid (Burst-forming unit [BFU-E] + colony-forming unit [CFU-E]) to granulocyte-monocyte (GM) generation, remained equivalent to *AAVS1* but significantly decreased in βE1 editing (Figure 2F). All these analyses indicate normal erythropoiesis in PRR-βE1 editing but not in βE1 editing.

We next compared the HbF induction by PRR-βE1 and Sicilian HPFH with well-characterized targets: the BCL11A erythroid-specific enhancer and BCL11A-binding site in the *HBG* promoter that have advanced into clinical studies.[12,26] Gene-editing efficiencies and the ratio of erythroid to GM colonies were comparable for all these targets (Figures 2G and S4G). All four targets produced HbF^{+ve} cells, with

Figure 2. Robust γ-globin induction and β-globin silencing in the erythroblasts differentiated from PRR-βE1-edited HSPCs

(A) Percentage of gene editing in PRR, βE1, and PRR-βE1 gene-edited healthy donor HSPCs. Indels measured by Sanger sequencing and ICE analysis. Deletion + Inversion (Del+Inv) (red checker box) in PRR-βE1 quantified by ddPCR. The PRR-βE1-edited cells had deletion, indels at PRR region and βE1. Donor = 5, n = 11. (B) FACS analysis of percentage of HbF^{+ve} cells in erythroblasts generated from gene-edited HSPCs. Gene-editing targets are indicated at the bottom. Control refers to unedited cells. Each dot indicates an individual experiment. Donor = 5, n = 11. (C) Percentage of fetal hemoglobin (HbF) tetramer as measured by variant HPLC for HSPCs gene edited for PRR, βE1, and PRR-βE1 and differentiated into erythroblasts. Donor = 3, n = 4. (D) Representative western blot image showing the band intensity of globin chains for erythroblasts derived from control, PRR, βE1, and PRR-βE1 gene-edited HSPCs. The editing in PRR and βE1 indicates the percentage of indels by ICE analysis and for PRR- βE1 edited, the percentage of editing includes the deletion + inversion quantified by ddPCR, cut site A and cut site B indels by ICE analysis. Donor = 1, n = 3. (E) Percentage of reticulocytes generated on erythroid differentiation of HSPCs gene edited for PRR, βE1, and PRR-βE1. Flow cytometric analysis of reticulocytes percentage was quantified on day 20 of three-phase erythroid differentiation. Donor = 5, n = 11. (F) Ratio of erythroid (E) to granulocyte-monocyte (GM) CFU colonies. HSPCs were gene edited for *AAVS1*, PRR, βE1, and PRR-βE1 and plated in methocult medium. Both BFU-E and CFU-E colonies were considered as erythroid (E) colonies. Donor = 2, n = 10. (G) Percentage of gene manipulation as measured by ddPCR for quantifying deletions in PRR-βE1 and Sicilian HPFH. Indel analysis of *AAVS1*, BCL11A enhancer, and HBG promoter by ICE analysis. Donor = 2, n = 4. (H) FACS analysis of percentage of HbF^{+ve} cells in erythroblasts generated from PRR-βE1, Sicilian HPFH, BCL11A enhancer, and HBG promoter. Donor = 2, n = 4. (I) Representative hemoglobin variant HPLC chromatograms showing HbF and HbA tetramers in gene-edited cells. (J) Percentage of HbF tetramers. HSPCs were gene edited for PRR-βE1, Sicilian HPFH, BCL11A enhancer, and HBG promoter, differentiated into erythroblasts and analyzed by variant HPLC. Donor = 2, n = 4. (K) Percentage of HbA tetramers. HSPCs were gene edited for PRR-βE1, Sicilian HPFH, BCL11A enhancer, and HBG promoter, differentiated into erythroblasts and analyzed by variant HPLC. Donor = 2, n = 4. (L) Representative western blot image showing the band intensity of globin chains for erythroblasts derived from PRR-βE1, Sicilian HPFH, BCL11A enhancer, and HBG promoter gene edited HSPCs. The editing in *AAVS1*, BCL11A enhancer, and HBG promoter indicates the indels quantified by ICE analysis. For PRR-βE1 and Sicilian HPFH, editing indicates the percentage of deletion and inversion quantified by ddPCR excluding the cut site indels. Donor = 1, n = 2. Error bars represent mean ± SEM, *$p \leq 0.05$, **$p \leq 0.01$, ***$p \leq 0.001$, ****$p \leq 0.0001$ (one-way ANOVA followed by Dunnett's multiple comparisons test).

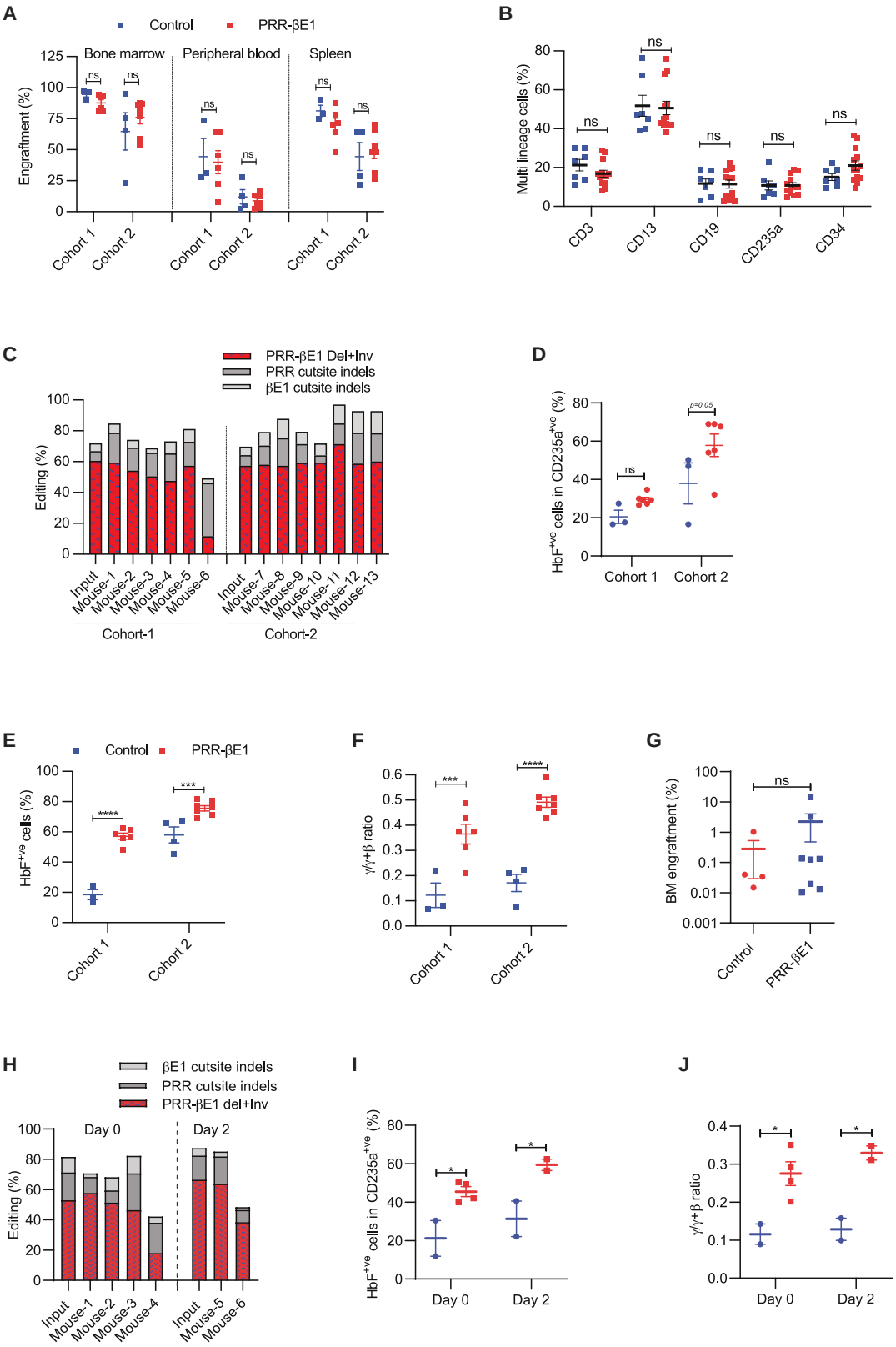

(legend on next page)

PRR-βE1 cells producing the highest proportion of HbF^{+ve} cells (Figure 2H). PRR-βE1-edited cells produced HbF tetramers that were 2-fold higher than the other targets and HbA tetramers were 3-fold lower (Figures 2I–2K). Western blot analysis further confirmed that PRR-βE1 editing increased γ-globin chains and decreased β-globin chains relative to other targets tested (Figures 2L and S4H). The γ-globin levels in PRR-βE1-edited cells were also higher in comparison with the HBB(-250)-βE1 (Figure S4I).

PRR-βE1 gene-edited HSPCs repopulate for long-term and generate HbF^{+ve} cells *in vivo*

To characterize the *in vivo* reconstitution capability of PRR-βE1 gene-edited cells, we used NBSGW mice, which support robust human cell engraftment and erythropoiesis.[27] Gene editing was performed on HSPCs from two healthy donors using PRR-βE1 and CRISPR RNA (crRNA) less RNP (control). The crRNA-free RNPs do not induce DNA double-strand breaks and therefore serve as an ideal control for assessing engraftment defects associated with Cas9 gene editing. The edited cells were transplanted into NBSGW mice as two cohorts, each infused with different donor cells and analyzed 16 weeks post transplantation.

The engraftment of PRR-βE1-edited cells in the bone marrow, peripheral blood, and spleen of the mice was comparable with that of the control group (Figures 3A and S5A). The multilineage repopulation potential of engrafted cells was also comparable among the groups (Figure 3B). The percentage of $CD235a^{+ve}$ erythroblasts was also similar, confirming the intact erythropoiesis *in vivo* from PRR-βE1-edited HSPCs. Importantly, genotyping of the long-term repopulating cells in all the mice revealed the retention of PRR-βE1 editing, and the percentage of editing was comparable with that of infused cells in 12 of the 13 animals tested (Figure 3C). Next, human $CD235a^{+ve}$ erythroblasts were sorted from mouse bone marrow and were found to be increased in the proportion of HbF^{+ve} cells *in vivo* following PRR-βE1 editing (Figure 3D). Furthermore, *in vitro* erythroid differentiation of cells retrieved from mouse bone marrow showed a significant increase in HbF^{+ve} cells (Figure 3E), γ/(γ+β) ratio (Figure 3F) and decreased β/(γ+β) ratio (Figure S5B) along with comparable reticulocyte production (Figure S5C).

To assess the serial repopulation potential of HSCs harboring PRR-βE1 editing, we infused bone marrow cells of primary recipients (cohort 2) to secondary recipients and analyzed the bone marrow 14 weeks post infusion. The analysis showed similar frequencies of engraftment of PRR-βE1-edited cells and control edited in the secondary recipients (Figure 3G).

PRR-βE1 gene editing without *ex vivo* culturing of HSPCs

Unlike lentiviral transduction or HDR-based gene editing, cytokine pre-stimulation of HSPCs may not be necessary for NHEJ-mediated gene editing. To examine whether PRR-βE1 gene editing is feasible without culture and cytokine pre-stimulation, HSPCs were electroporated immediately following purification and infused into NBSGW mice. The strategy was compared with the standard protocol, which consists of 48 h of cytokine stimulation prior to electroporation. On analysis after 16 weeks post transplantation, both groups exhibited comparable levels of bone marrow engraftment and PRR-βE1 gene editing (Figures 3H and S5D). The multilineage repopulation potential of engrafted cells between the *AAVS1* control and PRR-βE1-edited cells remained comparable (Figure S5E). Functionally, PRR-βE1-edited HSPCs from both uncultured and cultured HSPCs produced significantly more HbF^{+} cells *in vivo* (Figure 3I), corroborating earlier findings. Furthermore, *in vitro* erythroid differentiation of cells from mouse bone marrow showed a significant increase in HbF^{+ve} cells (Figure S5F) and γ/(γ+β) ratio (Figure 3J) and decreased β/(γ+β) ratio (Figure S5G) in PRR-βE1-edited cells compared with the *AAVS1* control.

PRR-βE1 gene-edited patient HSPCs reverse SCD phenotype

To test the potential of our PRR-βE1 gene-editing strategy in the reversal of the sickle phenotype, the plerixafor-mobilized HSPCs from two SCD patients of compound heterozygous genotype HbS/CD41/CD42(-TCTT) and HbS/IVS1-5 (Figure S6A) were gene edited with Cas9-RNPs targeting *AAVS1*, PRR, βE1, and PRR-βE1. The gene-editing frequency in each condition was >80%, with a PRR-βE1 deletion frequency of >56% (Figure 4A). The gene-edited cells were *in vitro* differentiated into erythroblasts under hypoxia (5% O_2)[28] and the erythroblasts derived from PRR-βE1 and βE1 gene-edited HSPCs showed a significant increase in the γ-globin mRNA expression (Figure 4B) and the percentage of HbF^{+ve} cells (Figure 4C).

Figure 3. PRR-βE1 gene-edited HSPCs repopulate for long-term and generate HbF^{+ve} cells *in vivo*

Control and PRR-βE1 gene-edited healthy donor HSPCs were transplanted into NBSGW mice and analyzed 16 weeks post transplantation (A–G). Each dot indicates a single mouse. Donor = 2. Each cohort indicates an independent experiment infused with HSPCs gene edited for PRR-βE1. Error bars represent mean ± SEM, ns, nonsignificant. ***$p \leq 0.001$, ****$p \leq 0.0001$ (two-way ANOVA followed by Dunnett's test). (A) Percentage of engraftment in the bone marrow, peripheral blood, and spleen calculated flow cytometrically using hCD45 and mCD45.1 markers. (B) Percentage of HSPC and lineage markers in bone marrow (BM) – CD3 (T cells), CD13 (monocyte), CD19 (B cells), CD235a (erythroid), and CD34 (HSPCs) in engrafted cells. $CD235a^{+}$ cells were analyzed form $CD45^{-}$ cells. (C) Percentage of PRR-βE1 deletion+inversion (Del+Inv), PRR cut site indels, and βE1 cut site indels in PRR-βE1 gene-edited HSPCs in infused fraction and in engrafted cells. (D) Percentage of HbF^{+ve} cells in $hCD235a^{+ve}$ cells obtained from mouse BM. (E) Percentage of HbF^{+ve} cells generated by erythroid differentiation of engrafted cells in the BM. (F) Ratio of γ/γ+β chains. Mouse BM was collected, *in vitro* differentiated into erythroblasts and analyzed by chain HPLC. (G) Percentage of engraftment in BM of secondary recipients analyzed 14 weeks post transplantation. *AAVS1* and PRR-βE1 gene-edited healthy donor HSPCs were gene edited immediately after CD34 purification (day 0) and 48 h post CD34 purification (day 2) and transplanted into NBSGW mice and analyzed 16 weeks post transplantation (G)–(J). Each dot indicates a single mouse. Donor = 1. Error bars represent mean ± SEM, ns, nonsignificant. *$p \leq 0.05$ (two-way ANOVA followed by Dunnett's test). (H) Percentage of PRR-βE1 deletion+inversion (Del+Inv), PRR cut site indels, and βE1 cut site indels in PRR-βE1 gene-edited HSPCs in Day 0 and Day 2 edited input fraction and in engrafted cells. (I) Percentage of HbF^{+ve} cells in $hCD235a^{+ve}$ cells obtained from mouse BM. (J) Ratio of γ/γ+β chains. Mouse BM was collected, *in vitro* differentiated into erythroblasts, and analyzed by chain HPLC.

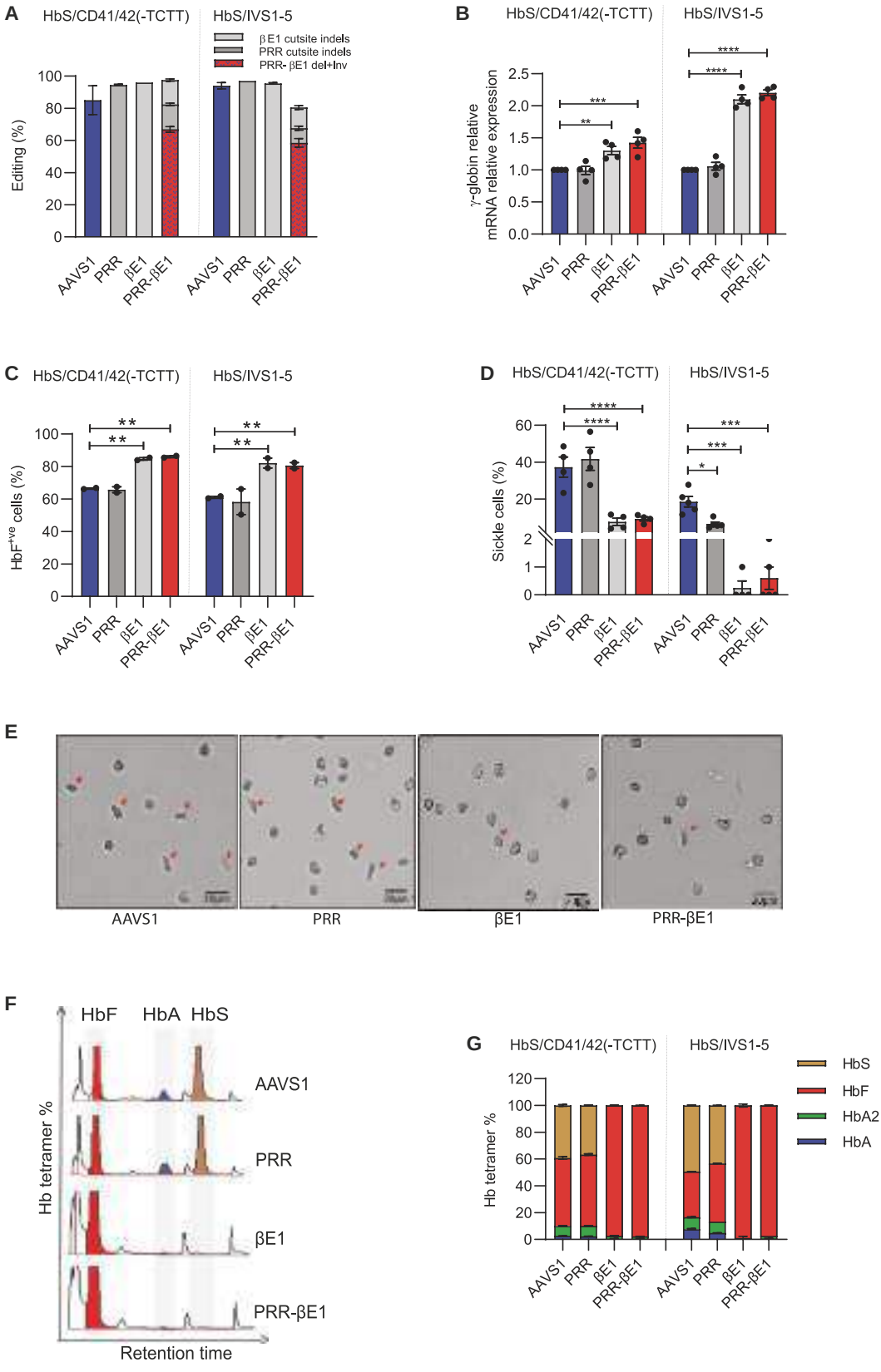

(legend on next page)

Further, we performed a sickling assay by treating reticulocytes with sodium metabisulfite. Upon treatment, control and PRR edited cells underwent sickling, whereas the βE1 and PRR-βE1-edited groups had a 12-fold (HbS/CD41/CD42(-TCTT)) and 30-fold (HbS/IVS1-5) reduction in sickling, respectively (Figures 4D and 4E). Variant HPLC analysis further showed that all the hemoglobin in the βE1 and PRR-βE1-edited cells was composed of HbF tetramers with nearly complete reduction of HbS (Figures 4F and 4G).

PRR-βE1 gene-edited patient HSPCs reverse β-thalassemia phenotype

To test the therapeutic potential of our gene-editing strategy in reversing β-thalassemia defects, we edited HSPCs obtained from β-thalassemia patients of three different β^0/β^0 genotypes: CD26 (G>A)/IVS1-5 (G>C), IVS1-5 (G>C), and CD30 (G>A) (Figure S6B). These β-thalassemia mutations are highly prevalent in India and Southeast Asian countries.[29,30] Due to poor peripheral blood mononuclear cell (PBMNC) yield, CD26 (G>A)/IVS1-5 (G>C) PBMNCs were differentiated into erythroblasts and edited on day 8 of erythroid differentiation. The PRR-βE1 gene-editing efficiency remained >80% in all the genotypes (Figure 5A). In *in vitro* erythropoiesis, βE1 and PRR-βE1 cells showed a significant increase in the frequency of HbF^{+ve} cells (Figure S7A) and γ/(γ+β) ratio (Figure S7B) and decrease in β/(γ+β) ratio (Figure S7C). The ratio of α to non-α-globin chains was also observed to be reduced (Figures 5B and 5C), suggesting the reduction of free α-globin chains. Western blot analysis of CD30 (G>A) gene-edited cells further confirmed that PRR-βE1 editing resulted in enhanced induction of γ-globin chains (Figures 5D and S7D).

Ineffective erythropoiesis, the classical phenotype of β-thalassemia, results from increased reactive oxygen species (ROS) levels, apoptosis of erythroid progenitors, and reticulocyte maturation arrest.[4,31] Erythroblasts originated from the PRR-βE1 gene-edited group showed a modest decrease in ROS levels (Figure S7E), a decrease in the proportion of apoptotic erythroblasts (stained by Annexin V) (Figures 5E and 5F), and importantly, a 3-fold increase in reticulocyte generation (Figures 5G and 5H) compared with the control. All these findings suggest that PRR-βE1 gene editing functionally rescues erythropoiesis in β-thalassemia by robust activation of γ-globin and silencing of defective β-globin (Figure S9).

PRR-βE1 gene-edited HSPCs have intact genome integrity

Reportedly, Cas9-generated DNA double-strand breaks pose a risk of genome-wide effects, such as genomic rearrangements.[32,33] Using HSPCs with micronuclei as a readout for cells with genomic instability, we microscopically evaluated individual HSPCs. In these experiments, we edited HSPCs using HiFi-Cas9, which has been demonstrated to minimize off-target editing and off-target mediated translocation.[33,34] HiFi-Cas9 retained the same frequency of on-target gene editing obtained in our earlier experiments with wild-type Cas9 (Figure 6A). Mitomycin C, an interstrand crosslinker that induces chromosomal rearrangements, was used as positive control. The frequency of micronuclei-positive HSPCs in PRR-βE1-edited HSPCs was not significantly greater than in unedited control HSPCs (Figure 6B).

As a second method, we employed array-based KaryoStat analysis to identify chromosomal abnormalities. The edited HSPCs were expanded for 7 days to magnify any potential defect. The whole-genome coverage analysis with a resolution of >1 Mb revealed that the PRR-βE1 gene-edited HSPCs exhibited neither loss nor gain of chromosomal copy number (Figure 6C).

To analyze genomic integrity with the highest resolution possible, we performed chromosomal aberrations analysis by single-targeted ligation-mediated PCR sequencing (CAST-Seq), which is sensitive enough to detect a single translocation event in 10,000 cells and can classify the type of structural variation.[33] CAST-Seq detects chromosomal abnormalities caused by on-target editing as well as the fusion of off-target edited sites to the on-target region. Upon gene editing HSPCs with HiFi-Cas9, CAST-Seq identified a single off-target-mediated translocation event between chr16: 684705–685217, which codes for the 3′- untranslated region (UTR) of WD repeat domain 24 (WDR24), and the on-target site (Figure 6D). This translocation was identified in two of our four CAST-Seq runs. The number of unique footprints (CAST-Seq hits), which testify to this translocation, is very low (13 hits) compared with the cumulated 58,897 on-target hits. This indicates that this particular translocation is an ultra-rare event, happening at a frequency close to the lower limit of detection of CAST-Seq (i.e., 0.01%). No homology-mediated translocation events were identified in the modified HSPCs. All these experiments indicate that chromosomal abnormalities occurred at very low frequency and the PRR-βE1 gene editing does not majorly compromise the integrity of the genome.

Figure 4. PRR-βE1 gene-edited patient HSPCs reverses sickle cell disease phenotype

Plerixafor-mobilized HSPCs from sickle cell patients of genotype HbS/CD41/42(-TCTT) and HbS/IVS1-5 were gene edited for *AAVS1*, PRR, βE1, and PRR-βE1. Error bars represent mean ± SEM. *$p \leq 0.05$, **$p \leq 0.01$, ***$p \leq 0.001$, ****$p \leq 0.0001$ (two-way ANOVA followed by Dunnett's test). (A) Percentage of gene editing. Indels measured by Sanger sequencing and ICE analysis. Deletion/inversion (Del+Inv) (red checker box) in PRR-βE1 quantified by ddPCR. The indels in the PRR-βE1 edited cells (gray checker box) were assessed using ICE analysis. Donor = 2, n = 4. (B) Relative globin mRNA expression. The patient HSPCs were gene edited for PRR, βE1, and PRR-βE1 and differentiated into erythroblasts. Real-time PCR analysis was used for mRNA quantification and the globin chain expression was normalized with β-actin. The patient genotype is indicated at the bottom. Donor = 2, n = 4. (C) Percentage of HbF^{+ve} cells. The gene-edited patient HSPCs were differentiated into erythroblasts and intracellular HbF positive cells were analyzed by FACS. Donor = 2, n = 4. (D) Percentage of sickle cells. Gene-edited patient HSPCs were differentiated into erythroblasts in hypoxia (5% O2) and the FACS sorted reticulocytes were treated with 1.5% sodium metabisulfite. Cells were scored from random fields using EVOS FL Auto Imaging System microscope. At least eight fields were analyzed. Each field contained a minimum of 150 cells. Donor = 2, n = 4. (E) Representative image of sickle cells (red arrow) and non-sickled cells. (F) Representative variant HPLC chromatogram showing HbA, HbF, and HbS. Donor = 2, n = 4. (G) Proportion of hemoglobin tetramer. The gene-edited patient HSPCs were differentiated into erythroblasts and the hemoglobin tetramers were analyzed by variant HPLC. Donor = 2, n = 4.

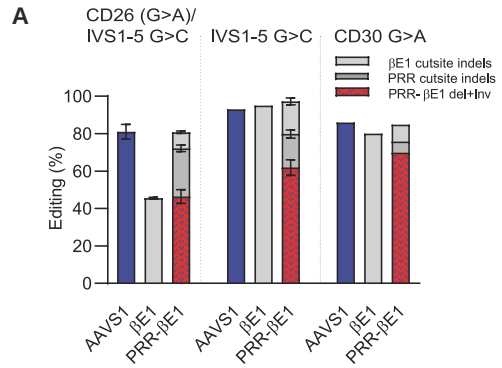

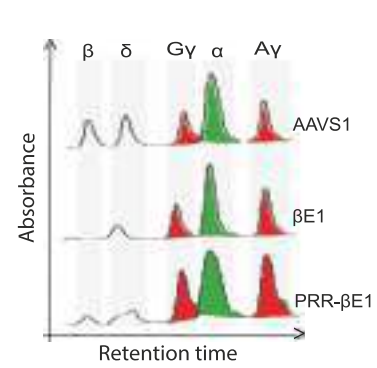

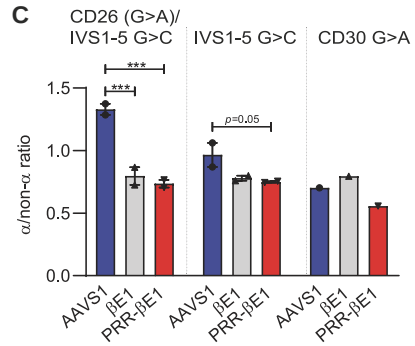

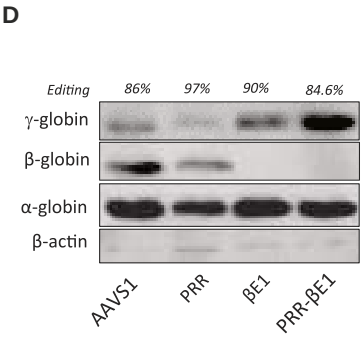

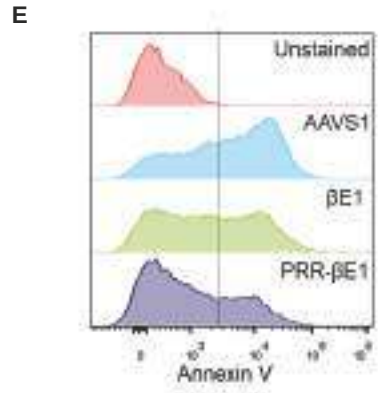

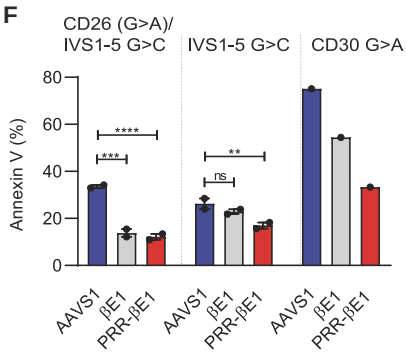

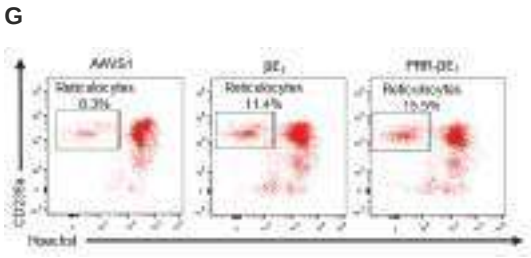

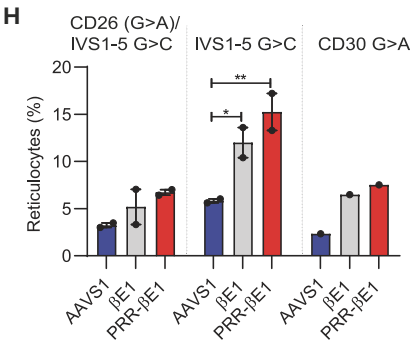

(legend on next page)

PRR-βE1 gene editing reconfigures chromosome looping and alters globin expression

Long-range chromatin interaction of the locus control region (LCR) and the promoters in the β-globin cluster regulate developmental stage-specific expression of globin genes.[35] To test the potential impact of PRR-βE1 gene editing on the configuration of the β-globin cluster, we employed a circular chromosome conformation capture (4C) assay. An interaction between hypersensitive site 1 (HS1) within the LCR and the *HBG2* promoter was observed in HUDEP-2 control cells. However, this interaction was enhanced in HUDEP-2 clones harboring a PRR-βE1 biallelic deletion. Furthermore, the interaction between other HS sites and *HBG2* promoters was newly gained in PRR-βE1 deleted cells. (Figure 7A). These data suggests that genomic proximity between the LCR and the *HBG* gene increases upon PRR-βE1 deletions and thus reactivates γ-globin in edited cells.

Thereafter, to understand the *trans*-acting factors involved in β-globin reactivation in the PRR-βE1 gene-edited cells, transcriptome analysis was carried out using the erythroblasts generated *in vitro* from gene-edited HSPCs. This analysis confirmed the overexpression of *HBG1* and *HBG2* with simultaneous downregulation of *HBB*. HBG was not among the top 20 significantly upregulated candidates in βE1 and showed a distinct set of upregulated genes than PRR-βE1 (Figure 7B and S8A). This indicates that different pathways are involved in PRR-βE1 and βE1 editing for γ-globin activation, with βE1 editing resulting in a weaker level of γ-activation on comparison. Cluster per million (cpm) values for the globin transcripts obtained from RNA sequencing further support higher γ-globin induction on PRR-βE1 editing (Figure 7C).

The transcriptome analysis and the followed-up real-time PCR analysis indicated the overexpression of HBBP1 in PRR-βE1 gene-edited cells (Figure 7D). HBBP1 was recently implicated in γ-globin activation.[36] BGLT-3, which is reported to promote transcriptional assembly at the γ-globin promoter, was seen to be abundant in edited cells by RT-PCR (Figure 7E).[37] Our gene set enrichment analysis (GSEA) with the published gene sets for HPFH mutation[38] showed a high normalized enrichment score (NES) of 2.13 for PRR-βE1 gene-edited cells confirming that PRR-βE1 gene editing creates an HPFH phenotype (Figure S8B), whereas the βE1 gene-edited cells showed relatively weaker enrichment (NES = 1.5) (Figure S8C).

All these findings suggest that the γ-globin activation in PRR-βE1 gene-edited cells occurs through altered chromatin looping mediated by promoter competition for the LCR and is similar to the HPFH phenotype.

DISCUSSION

Genetic reactivation of developmentally silenced HbF has gained considerable attention as a potential therapy for the broad spectrum of β-hemoglobinopathies. In this study, we have identified the PRR-βE1 sequence as a core HbF regulatory region present in all the deletional HPFH mutations. When present, PRR-βE1 effectively reverses the cellular phenotype of both SCD and β-thalassemia major by disrupting the production of defective β-globin and concurrently inducing robust HbF production through LCR switching mechanism. We specifically showed that PRR-βE1 gene-edited HSPCs have sustained engraftment, repopulation fitness, and genome integrity, highlighting the potential of this approach for future clinical studies.

Among the naturally existing mutations that produce pancellular HbF, deletional HPFH mutations are highly prevalent and are shown to generate a high frequency of HbF^{+ve} RBCs.[13] Even a heterozygous deletion can result in an HbF level of 65.6% with 8.9 g/dL of hemoglobin on co-inheritance with β-thalassemia.[21] Identifying the core region in HPFH deletions will enable us to recreate the HPFH phenotype by gene editing only the core region. The PRR region is conserved in δβ-thalassemia but excised in HPFH deletions.[39] However, deletion of the PRR site alone did not activate the HbF in our studies, consistent with earlier observations.[39] Even a deletion of 10.5 kb spanning the PRR region to the region located before the β-globin promoter had little effect on γ-globin production. In contrast, disruption of βE1 alone induced γ-globin production. Shen et al. showed that the improved γ-globin levels obtained by disrupting the HBB gene and its regulatory region is not sufficient to compensate for the loss of β-globin.[40] Our results provide compelling evidence that simultaneous disruption of the PRR region and β-globin reactivates γ-globin robustly without negatively impacting the erythroid maturation. While PRR disruption ensures that δβ-thalassemia-like phenotype is not created and the βE1 cut site confirms that even in the case of inversion or indels, the β-globin gene expression gets ablated and is associated with γ-globin production: thus PRR-βE1 is a more potent target than the original Sicilian HPFH.

Figure 5. PRR-βE1 gene-edited patient HSPCs reverse β-thalassemia phenotype

The G-CSF mobilized HSPCs from β-thalassemia patients of genotype IVS1-5 (G>C), and CD30 (G>A) were gene edited for *AAVS1*, βE1, and PRR-βE1. For HbE (G>A)/IVS1-5 (G>C), the PBMNCs were differentiated into erythroblasts and gene edited for *AAVS1*, βE1, and PRR-βE1. Error bars represent mean ± SEM. *$p \leq 0.05$, **$p \leq 0.01$, ***$p \leq 0.001$ (two-way ANOVA followed by Dunnett's test). Donor = 3, n = 5. (A) Percentage of gene editing in HSPCs. Deletion/Inversion (Del+Inv) in PRR-βE1 as quantified by ddPCR. Indels of the cut sites PRR and βE1 were measured by ICE analysis. (B) Representative globin chain HPLC chromatograms. (C) α/non-α ratio in the erythroblasts generated from gene-edited HSPCs. (D) Representative western blot image showing the band intensity of globin chain erythroblasts derived from *AAVS1*, PRR, βE1, and PRR-βE1 gene-edited CD30 (G>A) patient HSPCs. Donor = 1, n = 1. The editing in PRR and βE1 indicates the percentage of indels in ICE analysis and for PRR-βE1 edited, the percentage of editing includes the deletion + inversion quantified by ddPCR, cut site A and cut site B indels by ICE analysis. Donor = 1, n = 1. (E) Representative flow cytometry image of Annexin V staining. (F) Percentage of Annexin V in the erythroblasts generated from gene-edited HSPCs. (G) Representative flow cytometry plots of reticulocytes marked by $CD235a^{+}$/$Hoechst^{-}$. (H) Percentage of reticulocytes generated from gene-edited HSPCs.

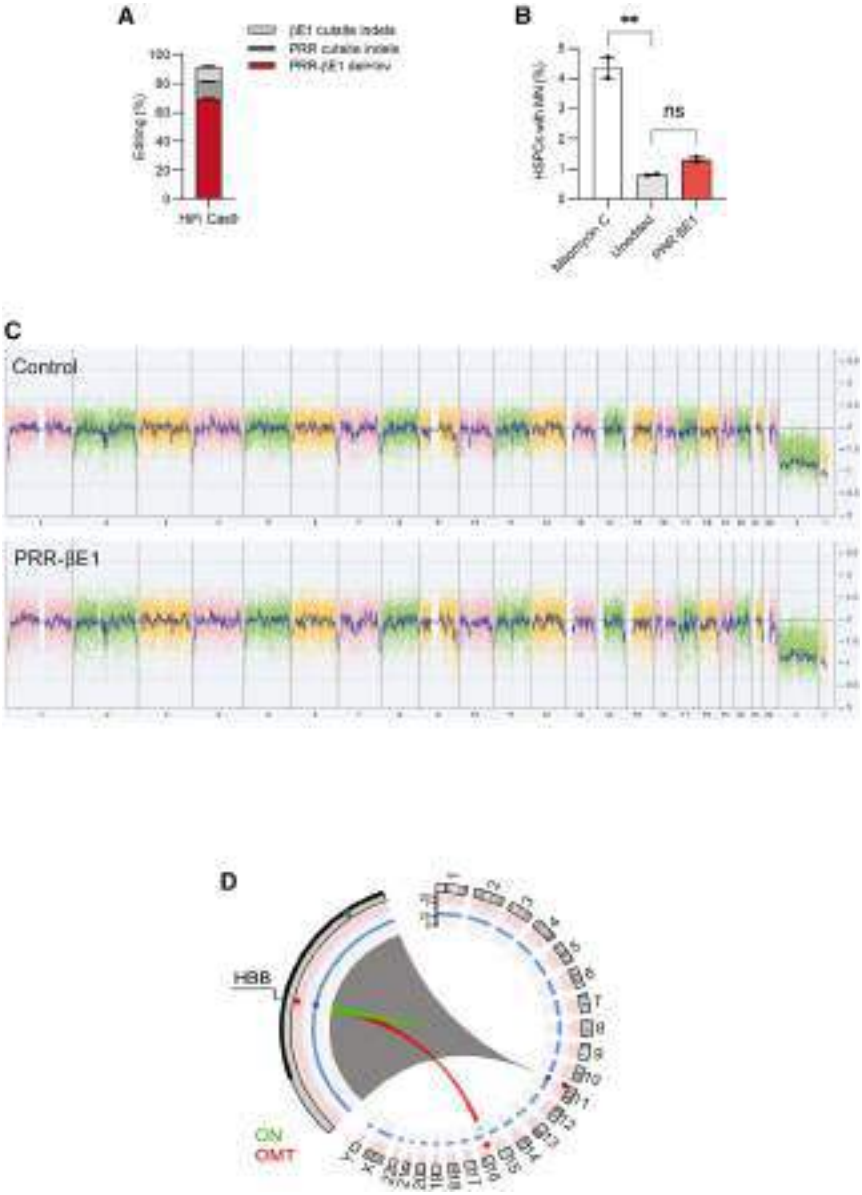

Figure 6. PRR-βE1 gene-edited HSPCs have intact genome integrity

(A) Percentage of gene editing on PRR-βE1 editing in healthy donor HSPCs using HiFi Cas9. Indels measured by Sanger sequencing and ICE analysis. Deletion/inversion (Del+Inv) (red checker box) in PRR-βE1 quantified by ddPCR. Donor = 1, n = 2. (B) Percentage of micronucleus (MN) in Mitomycin C treated, unedited, and PRR-βE1 gene-edited HSPCs scored 48 h post nucleofection after staining with Giemsa. Donor = 1, n = 2. (C) KaryoStat analysis of healthy donor HSPCs gene edited for PRR-βE1 deletion. Donor = 1, n = 2. (D) Circos plot showing off-target mediated translocation between the PRR-βE1 on-target site and βE1 off-target site in PRR-βE1 edited samples present in chr16 identified by CAST-Seq. Donor = 1, n = 4. Error bars represent mean ± SEM. ns, nonsignificant, **p ≤ 0.01 (one-way ANOVA followed by Dunnett's multiple comparisons test).

We observed a new genomic interaction between *HBG2* and a region downstream of *HBB* in PRR-βE1-edited cells (Figure 7A). Interestingly, this interaction site is deleted in Sicilian HPFH. Whether this region has a regulatory role on *HBG* expression and contributes to increased HbF in PRR-βE1 over Sicilian HPFH is to be explored.

While our manuscript was under preparation, two new articles provided deeper insight into the PRR-βE1 regulatory region. Topfer et al. analyzed both HPFH and δβ-thalassemia deletions and identified that the disruption of the β-globin promoter is sufficient for HbF reactivation.[19] One of our initial targets for editing, HBB(-250)-βE1, editing closely mimics the target analyzed by Topfer et al., and it had relatively less γ-globin activation over PRR-βE1 editing in our study (Figure S4I), and the region resembles British black and Croatian β-thalassemia genotypes.[24,25] βE1 gene-editing also disrupts the β-globin and reactivates the γ-globin, supporting the earlier findings.[19,41] The loss of β-globin reduces the levels of ATF4, which in turn decreases MYB and BCL11A to upregulate γ-globin.[41] This approach also resulted in decreased γ-globin activation than PRR-βE1 editing (Figures 2D, 5D, and 7C). Secondly, through a single-cell functional assay, Shen et al. demonstrated globin chain imbalance in erythroid colonies with β-globin (HBB-HBD$^{-/-}$) disruption but not in colonies with an *HBB-3.5kb* deletion that encompasses the PRR 3.5kb region, HBD, and HBB.[40] A long-range distal regulatory role has been proposed for the region upstream of HBD and this merges with the functional role of BCL11A in the HbF reactivation.[40]

Ramdier et al. reported a strategy of combining lentiviral transduction of anti-sickling β-globin and gene editing to disrupt endogenous β-globin, and enhance the proportion of anti-sickling hemoglobin.[42] This clearly depicts the competition between defective endogenous β-globin chains and exogenously supplemented globin chains for hemoglobin tetramer formation. In the ongoing clinical trial CLIMB SCD-121, HSPCs from SCD patients were gene edited for the BCL11A erythroid-specific enhancer; the gene-editing efficiency was up to 82.6%. HbF levels were 43.2% and the presence of HbS tetramers was up to 52.3%.[12] This indicates that, irrespective of the gene-editing efficiency and γ-globin activation efficacy, an intact β-globin regulatory region allows production of mutated β-globin chains at reduced levels. Similarly, in the BCL11A shRNA clinical trial, HbS constitutes up to 70% of hemoglobin tetramers.[11] The PRR-βE1-editing strategy directly excises the promoter and coding regions of β-globin, resulting in a major

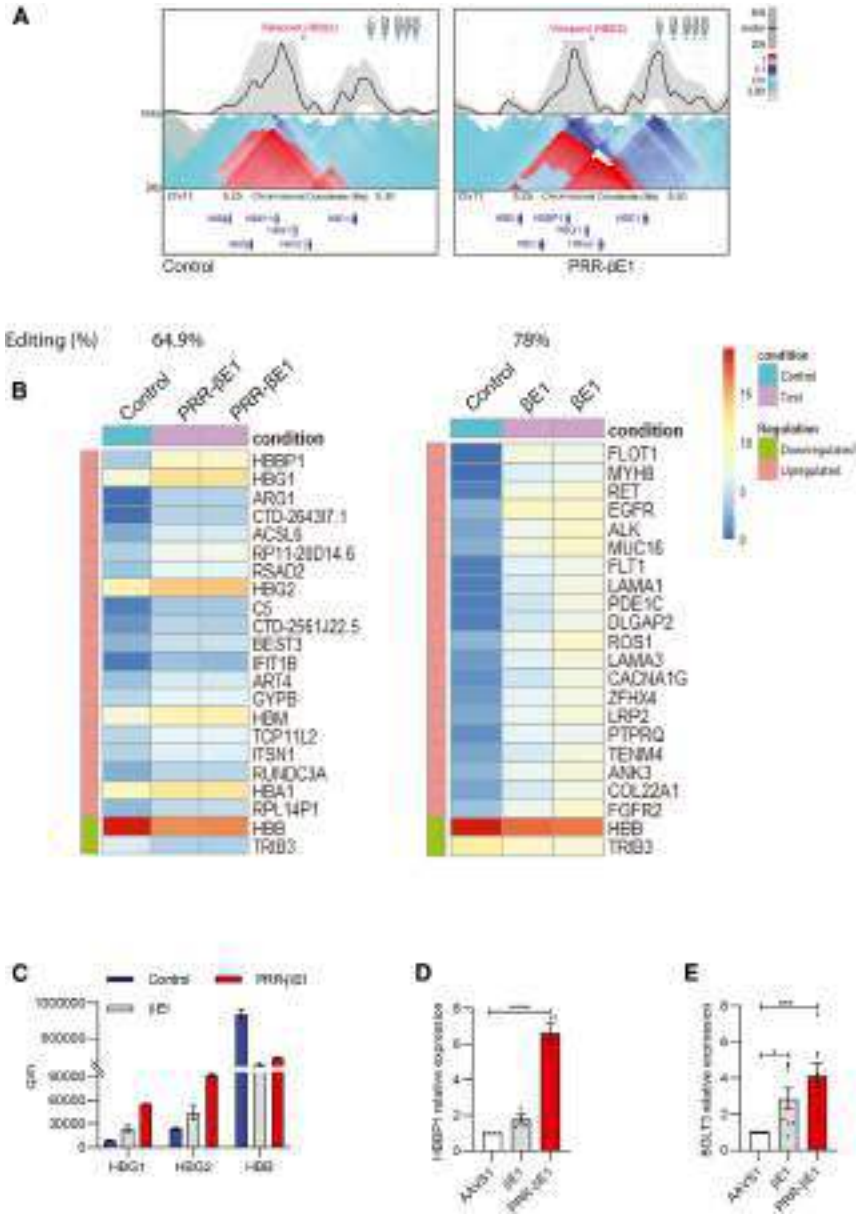

Figure 7. PRR-βE1 gene editing reconfigures chromosome looping and alters globin expression

(A) 4C analysis of single-cell sorted control and two PRR-βE1 biallelic gene-edited HUDEP-2 clones using *HBG2* promoter as a viewpoint. n = 4. (B) Heatmap of the top differentially expressed genes of erythroblasts derived from PRR-βE1 and βE1 gene-edited HSPC indicating the relative gene expression pattern of genes up- and downregulated compared with control. Donor = 1, n = 2. (C) Cluster per million (cpm) values for the globin transcripts obtained from RNA sequencing. (D) Relative HBBP1 mRNA expression in erythroblasts derived from βE1 and PRR-βE1 gene-edited HSPCs compared with *AAVS1*. The globin chain expression is normalized with β-actin. Donor = 1, n = 4. (E) Relative BGLT3 mRNA expression in erythroblasts derived from βE1, a PRR-βE1 gene-edited HSPC compared with *AAVS1*. The globin chain expression is normalized with β-actin. Donor = 2, n = 8. Error bars represent mean ± SEM.

reduction in the concentration of HbS, which will prevent the sickling of RBCs. This strategy will also be applicable for β-thalassemia, where the intact β-globin promoter drives production of truncated β-globin chains (Figure S9). Whether such an approach results in any free alpha globin levels is yet to be determined.

For a while, HPFH deletions were considered to be potential gene-editing targets. However, there were no reports on the genome integrity of the HSPCs and their ability to engraft post editing. HSPCs with a 4.9-kb deletion in the *HBG* promoter were shown to be lost post transplantation, and it was hypothesized that HSPCs having larger deletions are transplantation incompetent.[26,43] To our knowledge, this is the first study to demonstrate that HSPCs with large deletions can engraft and repopulate in both primary and secondary recipients. Our study also suggests that gene editing for large HPFH deletions is feasible without chromosomal aberrations when HiFi-Cas9 is used in conjunction with a carefully chosen single guide RNA (sgRNA). The gene-editing approach and the cytokine prestimulation that we described can potentially simplify the manufacturing process and reduce the cost associated with HSPC gene therapy.

In conclusion, our study sheds light on the crucial function of the PRR-βE1 region in regulating HbF and shows that this region is a key target for gene editing to activate fetal hemoglobin robustly to reduce mutated β-globin and to reverse major β-hemoglobinopathies phenotype. This study provides the first proof that large genomic sequences can be precisely modified in the HSPCs without endangering the multilineage repopulation potential and genome integrity.

MATERIALS AND METHODS

Purification and culture of CD34^{+ve} HSPCs

The unused G-CSF mobilized peripheral blood collected for allogeneic stem cell transplantation and Plerixafor-mobilized peripheral blood from SCD, or β-thalassemia patients were collected from transplantation unit of Christian Medical College, Vellore with prior institutional review board approval. The CD34^{+ve} HSPCs were purified as described in our previous studies.[44–46]

Electroporation of RNP complex in HUDEP-2, CD34^{+ve} cells and β-hemoglobinopathies patient HSPCs

SgRNAs were designed using CRISPR Design Tool (Synthego) and CRISPR-Cas9 guide RNA design checker (IDT), and the efficient gRNAs with least off-target sites were selected. List of gRNA used in the study is mentioned in Table S2. For nucleofection of HUDEP-2 cell lines, 100 pmol of Cas9 (Takara) was incubated at room temperature for 10 min with 200 pmol of sgRNA (Synthego). For dual sgRNA gene editing, 100 pmol of Cas9 RNP with cut site A sgRNA and 100 pmol of Cas9 RNP with cut site B sgRNA were nucleofected (Lonza 4D nucleofector) with CA137 pulse code. For electroporation of CD34^{+ve} HSPCs, 50 pmol of Cas9 RNP with sgRNA against PRR and 50 pmol of Cas9 RNP with sgRNA against βE1 were used; 2×10^5 cells were electroporated using P3 primary cell solution and supplement and were electroporated using Lonza 4D nucleofector with DZ100 pulse code.

For nucleofection of SCD and β-thalassemia patient HSPCs, 100 pmol of Cas9 (Takara) was incubated at room temperature for 10 min with 200 pmol of sgRNA (Synthego). For dual sgRNA gene editing 100 pmol of Cas9 RNP with cut site A sgRNA and 100 pmol of Cas9 RNP with cut site B sgRNA were nucleofected (Lonza 4D nucleofector) with DZ100 pulse code.

HUDEP-2 expansion and differentiation

The HUDEP-2 cells were cultured in StemSpan SFEM-II media containing SCF (50 ng/mL), EPO (3 U/mL), dexamethasone (1 μM), doxycycline (1 μg/mL), and glutamine (1x) at 2×10^5 cells/mL confluency with media change on alternative days. For erythroid differentiation, previously reported protocol with minor modifications was used.[47] The cells were seeded at a density of 2×10^5 cells/mL in IMDM GlutaMAX Supplement media containing 3% AB serum, 2% FBS, insulin (10 μg/mL), heparin (3U/mL), EPO (3U/mL), Holotransferrin (200 μg/mL), SCF (100 ng/mL), interleukin (IL)3 (10 ng/mL) and doxycycline (1 μg/mL). On day 2, cells were seeded at a cell density of 3.5×10^5 cells/mL. On day 4, the cells were seeded at a cell density of 5×10^5 cells/mL in the media containing the above-mentioned cytokine except doxycycline. On day 6, the cells were seeded at a cell density of 1×10^6 cells/mL in the media with all the components of day 4 media along with increased concentration of Holotransferrin (500 μg/mL). The cells were analyzed for HbF^{+ve} cells, differentiation profile, and globin chains using HPLC.

Erythroid differentiation of CD34^{+ve} HSPCs

The protocol for erythroid differentiation from CD34^{+ve} HSPCs was adopted from the literature with minor modifications.[48] The three-phase erythroid differentiation protocol involves culturing the CD34^{+ve} cells at a seeding density of 5×10^4 cells/mL in phase I from day 0 to day 8 with a media change on day 4. The phase I media is prepared using IMDM GlutaMAX Supplement media containing 5% AB serum, insulin (20 μg/mL), heparin (2 U/mL), EPO (3 U/mL), Holotransferrin (330 μg/mL), SCF (100 ng/mL), IL3 (50 ng/mL) and hydrocortisone (1 μg/mL). In phase II, the cells were seeded at a density of 2×10^5 cells from day 8 to day 12 in media containing all the components of phase I except hydrocortisone and IL3. In phase III, the cells were seeded at a density of 5×10^5 cells from day 12 to day 20 in media containing all the components of phase II except SCF with a media change on day 16. On day 20, the cells were collected for F^{+ve} cells analysis, differentiation marker analysis, and for hemoglobin and globin chain HPLC.

For differentiation of healthy donor and thalassemia patient HSPCs, the cells were cultured at 37°C, 5% CO_2 and in normoxia conditions (21% O_2). For the erythroid differentiation of SCD patient HSPCs, the above protocol was followed except the oxygen levels where we have cultured the SCD patient cells under hypoxic conditions (5% O_2) until day 20 to promote robust sickling of the erythroid differentiated cells.[28]

Flow cytometry

For HbF^{+ve} cell analysis, 1×10^5 erythroid differentiated cells were briefly washed with PBS and fixed with 0.05% glutaraldehyde for 10 min and permeabilized with 0.1% Triton X-100 for 5 min. The cells were stained with anti-HbF APC antibody (dilution 1:50) and were acquired and analyzed using Cytoflex LX Flow Cytometer (Beckmann Coulter) or AriaIII flow cytometer (BD Biosciences) and analyzed using FlowJo (BD Biosciences). For erythroid differentiation analysis, 1×10^5 cells from the terminal day of erythroid differentiation were stained for erythroid differentiation markers anti-CD71-FITC (dilution 1:33), anti-CD235a PE-Cy7 (dilution 1:50) and Hoechst 33342 (dilution 1:1,000). After 20 min of incubation in the dark, the cells were washed with PBS followed by analysis using Cytoflex LX Flow Cytometer (Beckmann Coulter) or AriaIII flow cytometer (BD Biosciences).

In vivo engraftment analysis

All the *in vivo* experiments in NBSGW mice models were conducted with approval from IAEC of Christian Medical College, Vellore, India. The NBSGW mice were bred in-house and were conditioned with busulfan at a concentration of 12.5 mg/kg of body weight, 48 h prior to the infusion.

CD34$^+$ HSPCs were pre-stimulated for 36 to 40 h with culture media containing appropriate cytokines and RUS cocktail[44,45]; 5×10^5 to 6×10^5 cells of control edited and PRR-βE1 edited were infused into NBSGW mice, immediately post electroporation. Sixteen to 18 weeks post infusion, the mice were euthanized and peripheral blood, bone marrow, and spleen were collected. After RBC lysis buffer incubation, the harvested cells were incubated with mouse Fc block and stained with hCD45 and mCD45 antibody. The % of engraftment is calculated using the formula (% hCD45/% hCD45 + % mCD45) × 100. In addition, the multilineage markers including CD19, CD3, CD13, and CD235a in bone marrow hCD45+ cells were also analyzed. For *ex vivo* erythroid differentiation, 3×10^6 cells were harvested from mouse bone marrow, seeded in erythroid differentiation media, and at the end of phase III of differentiation, the % of F^{+ve} cells, the differentiation profile, and globin chains were analyzed. For *in vivo* HbF^{+ve} cell analysis in NBSGW, 1×10^6 bone marrow cells

were stained with 10 μL of CD235a antibody and sorted based on the presence of immunophenotypic marker CD235a, followed by F^{+ve} cell analysis. For secondary infusion, 4×10^6 cells from the pooled fraction harvested from primary recipient bone marrow were infused to secondary recipients 48 h post busulfan conditioning. After 14 weeks, the mice were euthanized and the harvested cells were stained with hCD45 and mCD45 antibody for calculating the % of engraftment.

In vitro sickling assay

Sickling assay protocol was adopted from the literature with minor modifications.[28,49] The gene-edited SCD patient HSPCs were differentiated until day 20 of erythroid differentiation under hypoxia (5% O_2). On day 20 of erythroid differentiation, enucleated cells (reticulocytes) marked by $Hoechst^{-ve}$ were flow sorted. The flow sorted cells were resuspended with phase III erythroid differentiation medium and seeded in 24-well plates. Freshly prepared 1.5% sodium metabisulfite in 1x PBS were mixed with phase III media containing the reticulocytes in 1:1 ratio and incubated at 37°C for 1 h under hypoxia (5% O_2). After the incubation, the sides of the 24-well plate were covered with parafilm. Live cell images were acquired using EVOS FL Auto microscope. The percentage of sickle cells were calculated as number of sickle cells divided by the total number of cells.

Quantitative real-time PCR analysis

A total of 3×10^6 cells from the day 8 of $CD34^+$ HSPC and day 6 of HUDEP-2 erythroid differentiation were used for total RNA using an RNeasy Mini Kit (Qiagen). For reverse transcription using Primescript RT reagent kit (Takara Bio Inc.), 1 μg of extracted RNA was used according to the manufacturer's instructions. For quantitative PCR, the SYBR Premix Ex Taq II (Takara Bio) was used for quantifying the specific transcripts and analyzed with QuantStudio 6 Flex (Life Technologies). Primers used in qPCR analysis are mentioned in Table S5.

Colony formation assay

Forty-eight hours post electroporation, 5×10^2 HSPCs were seeded in 1.5 mL of Methocult Optimum (STEMCELL Technologies), and after 14 days, the colonies were scored based on the morphology as CFU-GM, CFU-GEMM, BFU-E, and CFU-E.

Droplet digital PCR

The frequency of large genomic deletions were quantified using EvaGreen-based ddPCR assay. The reaction mixture includes 20 ng of genomic DNA, 1x QX200 ddPCR EvaGreen supermix, and 100 nM primers for 20 μL reaction. For absolute measure of deletions, we designed primers that amplify the sequences flanking the cut sites after targeted deletion. Control primers amplifying embryonic globin gene were used as loading control (EG). The percentage of deletion was calculated using the following formula:

$$\left(\frac{EAB}{EE}\right) * 100$$

where,

EAB is DNA copies/μL from primers flanking the cut sites of edited samples, and EE is DNA copies/μL from primers amplifying embryonic globin gene of edited samples.

The second approach involves the quantification of the individual cut sites of the deletion, normalized with the read outs from the unedited control samples.

$$\left(100 - \left(\frac{EA * \left(\frac{UE}{UA}\right)}{EE}\right) + \left(\frac{EB * \left(\frac{UE}{UB}\right)}{EE}\right)\right) * 100$$

Where,

EA – DNA copies/μL from primers flanking the cut site A of edited samples.

EB – DNA copies/μL from primers flanking the cut site B of edited samples.

EE - DNA copies/μL from primers amplifying embryonic globin gene of edited samples.

UA – DNA copies/μL from primers flanking the cut site A of unedited samples.

UB – DNA copies/μL from primers flanking the cut site B of unedited samples.

UE - DNA copies/μL from primers amplifying embryonic globin gene of unedited samples.

The indels at the individual cutsite were quantified using ICE analysis with the primers mentioned in Table S3. Primers used in ddPCR analysis are mentioned in Table S4.

Hemoglobin and globin chain analysis using HPLC

The gene-edited HUDEP-2 cell lines and $CD34^{+ve}$ HSPCs were collected on day 8 and day 20 of erythroid differentiation, respectively. The cells were sonicated for 60 s with 50% AMP in ice using ultrasonicator (Vibra-Cell) and centrifuged at 14,000 rpm for 5 min at 4°C. For hemoglobin HPLC, the protein lysate was analyzed for hemoglobin tetramer using G8 HPLC Analyzer (Tosoh). The globin chain analysis was performed using HPLC equipment with UV detector (Shimadzu) and the analysis was performed using LC SolutionsTM software (Shimadzu) using the previously reported method.[50] Aeris Widepore 3.6 lm XB-C18 25 cm 4.6 mm column behind a Security Guard UHPLC Widepore C18 4.6 mm guard column (PhenomenexTM) is used for chromatographic separation of the analytes. HPLC conditions include 0.1% trifluoroacetic acid (TFA), pH 3.0 (solvent A), mobile phase - 0.1% TFA in acetonitrile

(solvent B) with gradient elution at a flow rate of 1.0 mL/min and column temperature maintained at 70°C with runtime around 8 min and UV detection range of 190 nm was set for globin chain detection.

Western blot analysis

Approximately 6×10^6 erythroblasts were collected on day 8 of erythroid differentiation. The lysates were prepared sonicating the cell pellets resuspended in RIPA buffer supplemented 1x protease and phosphatase inhibitor cocktail. Twenty micrograms of protein lysates resuspended in 1x Lamelli buffer were loaded to the wells of SDS-PAGE. The western blots were performed using the primary antibodies, anti-hemoglobin α (1:1,000 dilution), anti-hemoglobin β (1:1,000 dilution), anti-hemoglobin γ (1:1,000 dilution), and anti-actin (1:1,000 dilution) along with anti-mouse immunoglobulin (Ig) G horseradish peroxidase (HRP) secondary antibodies. Densitometric analysis of the globin bands were performed by normalizing with β-actin. List of western blot antibodies used in the study were mentioned in Table S7.

Transcriptome analysis

Total RNA was extracted using a Qiagen RNA isolation kit, quantified using Qubit RNA Assay HS, purity checked using QIAxpert, and RNA integrity was assessed on TapeStation using RNA HS ScreenTapes (Agilent, Cat# 5067-5579). NEB Ultra II Directional RNA-Seq Library Prep kit protocol was used to prepare libraries for total RNA sequencing (RNA-seq). Prepared libraries were quantified using Qubit High Sensitivity Assay (Invitrogen, Cat# Q32852). A cluster flow cell is loaded on Illumina HiSeq 4000 instrument to generate 60 M, 100 bp paired-end reads. Read Counts from mapped reads were obtained using Feature Counts. Differential expression analysis was performed using DESEQ2. GSEA was by GSEA software from the Broad Institute. A ranked list of differentially expressed genes from RNA-seq data was loaded into GSEA and tested against a list of genes documented from published reports. A heatmap for differentially regulated genes was generated using Morpheus (Broad Institute).

CAST-Seq analysis

CAST-Seq library preparation was performed as previously described.[33] Two technical replicates derived from two independent editing experiments were prepared and analyzed against a corresponding untreated control sample. We considered as relevant findings all sites identified in at least two out of four replicates with a read-to-CAST-Seq hit ratio of >10 to eliminate unspecific reads. CAST-Seq libraries were sequenced by NGS service provider Genewiz (part of Azenta Life Sciences). At Genewiz, sequencing was performed on an Illumina NovaSeq device collecting 2x 150 bp paired-end reads. The bioinformatics analysis was adapted to allow for concomitant input of more than one target site/guide RNA sequence. The oligo nucleotides used for CAST-Seq analysis are mentioned in Table S8.

Micronucleus assay

Micronucleus assay was performed as previously described[51] following the published guidelines.[52] Briefly, the gene-edited HSPCs were incubated with 10 μM cytochalasin B for 23 h and fixed with methanol and stained with Giemsa stain. The images were captured using ×40 magnification using an Olympus upright microscope BX43.

KaryoStat assay

Gene-edited HSPCs were collected for genomic DNA isolation using PureLink Genomic DNA Mini Kit (catalog #K182000) and quantified using Qubit dsDNA assay. After digestion of 250 ng of genomic DNA using Nsp I restriction enzyme, the DNA was ligated with adapter and amplified. The DNA was fragmented followed by labeling with biotin and the labeled DNA was hybridized onto GeneChip arrays. GeneChip Fluidics Station 450 were used for washing and staining of Chips simultaneously scanned using GeneChip Scanner 3000 7 G. Data were analyzed using ChAS 3.2. The raw data were processed using Genotyping Console v4.0 and Chromosome Analysis Suite 3.2 with NetAffx na33.1 (UCSC GRCh37/hg19), and the output data were interpreted with the UCSC Genome Browser (https://genome.ucsc.edu/; GRCh37/hg19 assembly).

4C analysis

4C was performed as per the protocol described in the literature with minor variations.[53] Cells (HUDEP-2 control and two PRR-βE1 clones harboring biallelic deletion) were fixed with fresh formaldehyde (1.5%) and quenched with glycine (125 mM) followed by washes with ice-cold PBS (2×) and pelleted and stored at −80°C. Lysis buffer (Tris-Cl pH 8.0 [10 mM], NaCl [10 mM], NP-40 [0.2%], PIC [1×]) was added to the pellets and were homogenized by Dounce homogenizer (15 stroked with pestle A followed by pestle B). The 3C digestion was performed with Csp6I (10 units, Thermofisher #ER0211) and ligation was performed by the T4 DNA ligase in 7.61 mL ligation mix (745 μL 10% Triton X-100, 745 μL 10x ligation buffer (500 mM Tris-HCl pH 7.5, 100 mM MgCl2, 100 mM DTT), 80 μL 10 mg/mL BSA, 80 μL 100 mM ATP, and 5.96 mL water). The ligated samples were de-crosslinked overnight then purified by PCI purification and subjected to ethanol precipitation and the pellet was eluted in TE (pH 8.0) to obtain the 3C library. The second 4C digestion was performed by DpnII (50 units, NEB) and the samples were ligated, purified, and precipitated similar to the 3C library to obtain the 4C library. The 4C library was subjected to RNAseA treatment and purified by the QIAquick PCR purification kit. The concentration of the library was then measured by Nanodrop and subjected to PCRs using the oligos for the respective viewpoints. The oligos used for the HBG2 viewpoint are mentioned in Table S6. The samples were PCR purified and subjected to next-generation sequencing with Illumina HiSeq2500 using 50-bp single-end reads. Data analysis was performed using 4Cseqpipe (https://github.com/changegene/4Cseqpipe) using default parameters.

DATA AVAILABILITY

RNA datasets are available in the Gene Expression Omnibus repository (GEO: GSE201346). 4C datasets are available in the Gene Expression Omnibus repository (GEO: GSE201388). All data are available in the main text or the supplemental information. Additional data

related to this paper may be requested from the corresponding author.

SUPPLEMENTAL INFORMATION

Supplemental information can be found online at https://doi.org/10.1016/j.omtn.2023.04.024.

ACKNOWLEDGMENTS

The authors thank the funders; Department of Biotechnology, government of India (BT/PR17316/MED/31/326/2015, BT/PR26901/MED/31/377/2017 and BT/PR31616/MED/31/408/2019 to ST), European Commission (HORIZON-RIA EDITSCD No. 101057659 to T.C.), ICMR-SRF fellowship (V.V., A.C.), CSIR-JRF fellowship (P.B.), and DST-INSPIRE fellowship (K.V.K.). The authors also thank Dr. Sowmya Pattabhi for help in designing the ddPCR strategy, Mr. Dhananjayan and Mr. Daniel Beno for ddPCR-related technical inputs, and the staffs of flow cytometry, animal facility, and core facilities for their support.

AUTHOR CONTRIBUTIONS

Conceptualization: S.T., A.S., S.V., S.M., and K.M. Experiment execution and analysis: V.V., A.C., M.R., P.B., M.A., K.W., B.S., S.S., K.V.K., A.J., S.R., A.P., Y.N., R.P., G.A. Technical supervision: S.T., A.S., D.N., S.V., P.B., S.M., M.B. Manuscript – review & editing: V.V., S.T., A.S., T.C., S.V., S.M., and K.M. Funding acquisition: S.T. and T.C.

DECLARATION OF INTERESTS

The authors declare no competing interests.

REFERENCES

1. De Sanctis, V., Kattamis, C., Canatan, D., Soliman, A.T., Elsedfy, H., Karimi, M., Daar, S., Wali, Y., Yassin, M., Soliman, N., et al. (2017). β-thalassemia distribution in the old world: an ancient disease seen from a historical standpoint. Mediterr. J. Hematol. Infect. Dis. *9*, e2017018.
2. Colah, R., Italia, K., and Gorakshakar, A. (2017). Burden of thalassemia in India: the road map for control. Pediatr. Hematol. Oncol. J. *2*, 79–84.
3. Boonyawat, B., Monsereenusorn, C., and Traivaree, C. (2014). Molecular analysis of beta-globin gene mutations among Thai beta-thalassemia children: results from a single center study. Appl. Clin. Genet. *7*, 253–258.
4. Origa, R. (2017). β-Thalassemia. Genet. Med. *19*, 609–619.
5. Sundd, P., Gladwin, M.T., and Novelli, E.M. (2019). Pathophysiology of sickle cell disease. Annu. Rev. Pathol. *14*, 263–292.
6. Fitzhugh, C.D., Hsieh, M.M., Allen, D., Coles, W.A., Seamon, C., Ring, M., Zhao, X., Minniti, C.P., Rodgers, G.P., Schechter, A.N., et al. (2015). Hydroxyurea-increased fetal hemoglobin is associated with less organ damage and longer survival in adults with sickle cell anemia. PLoS One *10*, e0141706.
7. Musallam, K.M., Sankaran, V.G., Cappellini, M.D., Duca, L., Nathan, D.G., and Taher, A.T. (2012). Fetal hemoglobin levels and morbidity in untransfused patients with β-thalassemia intermedia. Blood *119*, 364–367.
8. Nuinoon, M., Makarasara, W., Mushiroda, T., Setianingsih, I., Wahidiyat, P.A., Sripichai, O., Kumasaka, N., Takahashi, A., Svasti, S., Munkongdee, T., et al. (2010). A genome-wide association identified the common genetic variants influence disease severity in β0-thalassemia/hemoglobin e. Hum. Genet. *127*, 303–314.
9. Masuda, T., Wang, X., Maeda, M., Canver, M.C., Sher, F., Funnell, A.P.W., Fisher, C., Suciu, M., Martyn, G.E., Norton, L.J., et al. (2016). Gene regulation: transcription factors LRF and BCL11A independently repress expression of fetal hemoglobin. Science *351*, 285–289.
10. Canver, M.C., Smith, E.C., Sher, F., Pinello, L., Sanjana, N.E., Shalem, O., Chen, D.D., Schupp, P.G., Vinjamur, D.S., Garcia, S.P., et al. (2015). BCL11A enhancer dissection by Cas9-mediated in situ saturating mutagenesis. Nature *527*, 192–197.
11. Esrick, E.B., Lehmann, L.E., Biffi, A., Achebe, M., Brendel, C., Ciuculescu, M.F., Daley, H., MacKinnon, B., Morris, E., Federico, A., et al. (2021). Post-transcriptional genetic silencing of BCL11A to treat sickle cell disease. N. Engl. J. Med. *384*, 205–215.
12. Frangoul, H., Altshuler, D., Cappellini, M.D., Chen, Y.-S., Domm, J., Eustace, B.K., Foell, J., de la Fuente, J., Grupp, S., Handgretinger, R., et al. (2021). CRISPR-Cas9 gene editing for sickle cell disease and β-thalassemia. N. Engl. J. Med. *384*, 252–260.
13. Ringelhann, B., Acquaye, C.T., Oldham, J.H., Konotey-Ahulu, F.I., Yawson, G., Sukumaran, P.K., Schroeder, W.A., and Huisman, T.H. (1977). Homozygotes for the hereditary persistence of fetal hemoglobin: the ratio of Gγ to Aγ chains and biosynthetic studies. Biochem. Genet. *15*, 1083–1096.
14. Cianetti, L., Care, A., Sposi, N.M., Giampaolo, A., Calandrini, M., Petrini, M., Massa, A., Marinucci, M., Mavilio, F., Ceccanti, M., et al. (1984). Association of heterocellular HPFH,-i-thalassaemia, and a 0-thalassaemia: haematological and molecular aspects. J. Med. Genet. *21*, 263–267.
15. Steinberg, M.H. (2020). Fetal hemoglobin in sickle hemoglobinopathies: high HbF genotypes and phenotypes. J. Clin. Med. *9*, 3782.
16. Venkatesan, V., Srinivasan, S., Babu, P., and Thangavel, S. (2020). Manipulation of developmental Gamma-globin gene expression: an approach for healing hemoglobinopathies. Mol. Cell Biol. *41*, e00253-20.
17. Ye, L., Wang, J., Tan, Y., Beyer, A.I., Xie, F., Muench, M.O., and Kan, Y.W. (2016). Genome editing using CRISPR-Cas9 to create the HPFH genotype in HSPCs: an approach for treating sickle cell disease and β-thalassemia. Proc. Natl. Acad. Sci. USA *113*, 10661–10665.
18. Antoniani, C., Meneghini, V., Lattanzi, A., Felix, T., Romano, O., Magrin, E., Weber, L., Pavani, G., El Hoss, S., Kurita, R., et al. (2018). Induction of fetal hemoglobin synthesis by CRISPR/Cas9-mediated editing of the human b-globin locus. Blood *131*, 1960–1973.
19. Topfer, S.K., Feng, R., Huang, P., Ly, L.C., Martyn, G.E., Blobel, G.A., Weiss, M.J., Quinlan, K.G.R., and Crossley, M. (2022). Disrupting the adult globin promoter alleviates promoter competition and reactivates fetal globin gene expression. Blood *139*, 2107–2118.
20. Joly, P., Lacan, P., Garcia, C., Couprie, N., and Francina, A. (2009). Identification and molecular characterization of four new large deletions in the β-globin gene cluster. Blood Cells Mol. Dis. *43*, 53–57.
21. Changsri, K., Akkarapathumwong, V., Jamsai, D., Winichagoon, P., and Fucharoen, S. (2006). Molecular mechanism of high hemoglobin F production in Southeast Asian-type hereditary persistence of fetal hemoglobin. Int. J. Hematol. *83*, 229–237.
22. Camaschella, C., Serra, A., Gottardi, E., Alfarano, A., Revello, D., Mazza, U., and Saglio, G. (1990). A new hereditary persistence of fetal hemoglobin deletion has the breakpoint within the 3' beta-globin gene enhancer. Blood *75*, 1000–1005.
23. Kulozik, A.E., Yarwood, N., and Jones, R.W. (1988). The Corfu αβ° thalassemia: a small deletion acts at a distance to selectively abolish β globin gene expression. Blood *71*, 457–462.
24. Anand, R., Boehm, C.D., Kazazian, H.H., Jr., and Vanin, E.F. (1988). Molecular characterization of a β0 -thalassemia resulting from a 1.4 kilobase deletion. Blood *72*, 636–641.
25. Dimovski, A.J., Efremov, D.G., Jankovic, L., Plaseska, D., Juricic, D., and Efremov, G.D. (1993). A β°-thalassaernia due to a 1605 bp deletion of the 5'β-globin gene region. Br. J. Haematol. *85*, 143–147.
26. Métais, J.Y., Doerfler, P.A., Mayuranathan, T., Bauer, D.E., Fowler, S.C., Hsieh, M.M., Katta, V., Keriwala, S., Lazzarotto, C.R., Luk, K., et al. (2019). Genome editing of HBG1 and HBG2 to induce fetal hemoglobin. Blood Adv. *3*, 3379–3392.
27. McIntosh, B.E., Brown, M.E., Duffin, B.M., Maufort, J.P., Vereide, D.T., Slukvin, I.I., and Thomson, J.A. (2015). Nonirradiated NOD,B6.SCID Il2rγ-/- Kit(W41/W41) (NBSGW) mice support multilineage engraftment of human hematopoietic cells. Stem Cell Rep. *4*, 171–180.
28. El Hoss, S., Cochet, S., Godard, A., Yan, H., Dussiot, M., Frati, G., Boutonnat-Faucher, B., Laurance, S., Renaud, O., Joseph, L., et al. (2020). Fetal hemoglobin rescues ineffective erythropoiesis in sickle cell disease. Haematologica *136*, 14–15.

29. Yang, Z., Cui, Q., Zhou, W., Qiu, L., and Han, B. (2019). Comparison of gene mutation spectrum of thalassemia in different regions of China and Southeast Asia. Mol. Genet. Genomic Med. *7*, 680.

30. Sinha, S., Black, M.L., Agarwal, S., Colah, R., Das, R., Ryan, K., Bellgard, M., and Bittles, A.H. (2009). Profiling β-thalassaemia mutations in India at state and regional levels: implications for genetic education, screening and counselling programmes. Hugo J. *3*, 51–62.

31. Arlet, J.-B., Ribeil, J.-A., Guillem, F., Negre, O., Hazoume, A., Marcion, G., Beuzard, Y., Dussiot, M., Moura, I.C., Demarest, S., et al. (2014). HSP70 sequestration by free α-globin promotes ineffective erythropoiesis in β-thalassaemia. Nature *514*, 242–246.

32. Leibowitz, M.L., Papathanasiou, S., Doerfler, P.A., Blaine, L.J., Sun, L., Yao, Y., Zhang, C.Z., Weiss, M.J., and Pellman, D. (2021). Chromothripsis as an on-target consequence of CRISPR–Cas9 genome editing. Nat. Genet. *53*, 895–905.

33. Turchiano, G., Andrieux, G., Klermund, J., Blattner, G., Pennucci, V., el Gaz, M., Monaco, G., Poddar, S., Mussolino, C., Cornu, T.I., et al. (2021). Quantitative evaluation of chromosomal rearrangements in gene-edited human stem cells by CAST-Seq. Cell Stem Cell *28*, 1136–1147.e5.

34. Kleinstiver, B.P., Pattanayak, V., Prew, M.S., Tsai, S.Q., Nguyen, N.T., Zheng, Z., and Joung, J.K. (2016). High-fidelity CRISPR–Cas9 nucleases with no detectable genome-wide off-target effects. Nature *529*, 490–495.

35. Vinjamur, D.S., Bauer, D.E., and Orkin, S.H. (2018). Recent progress in understanding and manipulating haemoglobin switching for the haemoglobinopathies. Br. J. Haematol. *180*, 630–643.

36. Ma, S.P., Xi, H.R., Gao, X.X., Yang, J.M., Kurita, R., Nakamura, Y., Song, X.M., Chen, H.Y., and Lu, D.R. (2021). Long noncoding RNA HBBP1 enhances γ-globin expression through the ETS transcription factor ELK1. Biochem. Biophys. Res. Commun. *552*, 157–163.

37. Ivaldi, M.S., Diaz, L.F., Chakalova, L., Lee, J., Krivega, I., and Dean, A. (2018). Fetal γ-globin genes are regulated by the BGLT3 long noncoding RNA locus. Blood *132*, 1963–1973.

38. Lamsfus-Calle, A., Daniel-Moreno, A., Antony, J.S., Epting, T., Heumos, L., Baskaran, P., Admard, J., Casadei, N., Latifi, N., Siegmund, D.M., et al. (2020). Comparative targeting analysis of KLF1, BCL11A, and HBG1/2 in CD34+ HSPCs by CRISPR/Cas9 for the induction of fetal hemoglobin. Sci. Rep. *10*, 10133.

39. Chung, J.E., Magis, W., Vu, J., Heo, S.-J., Wartiovaara, K., Walters, M.C., Kurita, R., Nakamura, Y., Boffelli, D., Martin, D.I.K., et al. (2019). CRISPR-Cas9 interrogation of a putative fetal globin repressor in human erythroid cells. PLoS One *14*, e0208237.

40. Shen, Y., Verboon, J.M., Zhang, Y., Liu, N., Kim, Y.J., Marglous, S., Nandakumar, S.K., Voit, R.A., Fiorini, C., Ejaz, A., et al. (2021). A unified model of human hemoglobin switching through single-cell genome editing. Nat. Commun. *12*, 4991.

41. Boontanrart, M.Y., Schröder, M.S., Stehli, G.M., Banović, M., Wyman, S.K., Lew, R.J., Bordi, M., Gowen, B.G., DeWitt, M.A., and Corn, J.E. (2020). ATF4 regulates MYB to increase γ-globin in response to loss of β-globin. Cell Rep. *32*, 107993.

42. Ramadier, S., Chalumeau, A., Felix, T., Othman, N., Aknoun, S., Casini, A., Maule, G., Masson, C., De Cian, A., Frati, G., et al. (2022). Combination of lentiviral and genome editing technologies for the treatment of sickle cell disease. Mol. Ther. *30*, 145–163.

43. Humbert, O., Radtke, S., Samuelson, C., Carrillo, R.R., Perez, A.M., Reddy, S.S., Lux, C., Pattabhi, S., Schefter, L.E., Negre, O., et al. (2019). Therapeutically relevant engraftment of a CRISPR-Cas9-edited HSC-enriched population with HbF reactivation in nonhuman primates. Sci. Transl. Med. *11*, eaaw3768.

44. Karuppusamy, K.V., Demosthenes, J.P., Venkatesan, V., Christopher, A.C., Babu, P., Azhagiri, M.K., Jacob, A., Ramalingam, V.V., and Rangaraj, S. (2022). The CCR5 gene edited CD34 + CD90 + hematopoietic stem cell population serves as an optimal graft source for HIV gene therapy. Front. Immunol. *13*, 1–15.

45. Christopher, A.C., Venkatesan, V., Karuppusamy, K.V., Srinivasan, S., Babu, P., Azhagiri, M.K.K., C, K., Bagchi, A., Rajendiran, V., Ravi, N.S., et al. (2021). Preferential expansion of human CD34+CD133+CD90+ hematopoietic stem cells enhances gene-modified cell frequency for gene therapy. Hum. Gene Ther. 1–33.

46. Venkatesan, V., Christopher, A.C., Karuppusamy, K.V., Babu, P., Kumar, M., Alagiri, K., and Thangavel, S. (2022). CRISPR/Cas9 gene editing of hematopoietic stem and progenitor cells for gene therapy applications. J. Vis. Exp. 1–20. https://doi.org/10.3791/64064.

47. Trakarnsanga, K., Griffiths, R.E., Wilson, M.C., Blair, A., Satchwell, T.J., Meinders, M., Cogan, N., Kupzig, S., Kurita, R., Nakamura, Y., et al. (2017). An immortalized adult human erythroid line facilitates sustainable and scalable generation of functional red cells. Nat. Commun. *8*, 14750–14757.

48. Chang, K.H., Smith, S.E., Sullivan, T., Chen, K., Zhou, Q., West, J.A., Liu, M., Liu, Y., Vieira, B.F., Sun, C., et al. (2017). Long-term engraftment and fetal globin induction upon BCL11A gene editing in bone-marrow-derived CD34+ hematopoietic stem and progenitor cells. Mol. Ther. Methods Clin. Dev. *4*, 137–148.

49. Zeng, J., Wu, Y., Ren, C., Bonanno, J., Shen, A.H., Shea, D., Gehrke, J.M., Clement, K., Luk, K., Yao, Q., et al. (2020). Therapeutic base editing of human hematopoietic stem cells. Nat. Med. *26*, 535–541.

50. Loucari, C.C., Patsali, P., Van Dijk, T.B., Stephanou, C., Papasavva, P., Zanti, M., Kurita, R., Nakamura, Y., Christou, S., Sitarou, M., et al. (2018). Rapid and sensitive assessment of globin chains for gene and cell therapy of hemoglobinopathies. Hum. Gene Ther. Methods *29*, 60–74.

51. Mosesso, P., and Cinelli, S. (2019). In vitro cytogenetic assays: chromosomal aberrations and micronucleus tests. Methods Mol. Biol. *2031*, 79–104.

52. Fenech, M., Chang, W.P., Kirsch-Volders, M., Holland, N., Bonassi, S., and Zeiger, E.; HUman MicronNucleus Project (2003). HUMN project: detailed description of the scoring criteria for the cytokinesis-block micronucleus assay using isolated human lymphocyte cultures. Mutat. Res. *534*, 65–75.

53. Van De Werken, H.J.G., Landan, G., Holwerda, S.J.B., Hoichman, M., Klous, P., Chachik, R., Splinter, E., Valdes-Quezada, C., Öz, Y., Bouwman, B.A.M., et al. (2012). Robust 4C-seq data analysis to screen for regulatory DNA interactions. Nat. Methods *9*, 969–972.

HGT

Preferential Expansion of Human CD34$^+$CD133$^+$CD90$^+$ Hematopoietic Stem Cells Enhances Gene-Modified Cell Frequency for Gene Therapy

Abisha Crystal Christopher,[1,†] Vigneshwaran Venkatesan,[1,2,†] Karthik V. Karuppusamy,[1,2] Saranya Srinivasan,[1] Prathibha Babu,[1,2] Manoj Kumar K. Azhagiri,[1,2] Karthik Chambayil,[1] Abhirup Bagchi,[1] Vignesh Rajendiran,[1] Nithin Sam Ravi,[1] Sanjay Kumar,[1] Srujan Kumar Marepally,[1] Kumarasamypet Murugesan Mohankumar,[1] Alok Srivastava,[1,3] Shaji R. Velayudhan,[1,3] and Saravanabhavan Thangavel[1,*,i]

[1]*Centre for Stem Cell Research (CSCR), A Unit of InStem Bengaluru, Christian Medical College Campus, Vellore, India;* [2]*Manipal Academy of Higher Education, Manipal, India;* [3]*Department of Hematology, Christian Medical College, Vellore, India.*

[†]*Equally contributing first authors.*

[i]*ORCID ID (https://orcid.org/0000-0001-6760-4106).*

CD34$^+$CD133$^+$CD90$^+$ hematopoietic stem cells (HSCs) are responsible for long-term multilineage hematopoiesis, and the high frequency of gene-modified HSCs is crucial for the success of hematopoietic stem and progenitor cell (HSPC) gene therapy. However, the *ex vivo* culture and gene manipulation steps of HSPC graft preparation significantly reduce the frequency of HSCs, thus necessitating large doses of HSPCs and reagents for the manipulation. In this study, we identified a combination of small molecules, Resveratrol, UM729, and SR1 that preferentially expands CD34$^+$CD133$^+$CD90$^+$ HSCs over other subpopulations of adult HSPCs in *ex vivo* culture. The preferential expansion enriches the HSCs in *ex vivo* culture, enhances the adhesion, and results in a sixfold increase in the long-term engraftment in NSG mice. Further, the culture-enriched HSCs are more responsive to gene modification by lentiviral transduction and gene editing, increasing the frequency of gene-modified HSCs up to 10-fold *in vivo*. The yield of gene-modified HSCs obtained by the culture enrichment is similar to the sort-purification of HSCs and superior to Cyclosporin-H treatment. Our study addresses a critical challenge of low frequency of gene modified HSCs in HSPC graft by developing and demonstrating a facile HSPC culture condition that increases the frequency of gene-modified cells *in vivo*. This strategy will improve the outcome of HSPC gene therapy and also simplify the gene manipulation process.

Keywords: hematopoietic stem cells, gene therapy, lentiviral, gene editing, HSC gene manipulation, long-term engraftment

INTRODUCTION

Gene modification of hematopoietic stem and progenitor cells (HSPCs) has opened new possibilities for autologous HSPC-based therapy compared to allogeneic HSPC therapy, which has several limitations.[1] The promising progress of lentiviral gene modification studies for β--hemoglobinopathies, primary immunodeficiency disorders, and lysosomal storage diseases[2–5] as well as gene-editing studies for β-hemoglobinopathies and HIV[6,7] highlight the therapeutic benefits of autologous HSPC gene therapy.

HSPC graft for gene manipulation is composed of lineage-committed progenitors marked by CD34$^+$CD133$^-$CD90$^-$, early progenitors (CD34$^+$CD133$^+$CD90$^-$), hematopoietic stem cells (HSCs) (CD34$^+$CD133$^+$CD90$^+$), and differentiated cells (CD34$^-$).[8] Lentiviral transduction requires a maximum of 48 h for prestimulation with cytokines followed by 24–48 h for viral transduction and 24 h for viral washout.[3,9–11] Similarly, gene editing requires 48 h for prestimulation and up to 24 h for relief from electroporation stress.[6,8,12] These steps demand 3–5 days of *ex vivo* culturing, compromising the stemness of gene-modified HSCs.

The loss of stemness associated with *ex vivo* culturing and the toxicity associated with the manipulation procedure particularly by the high doses of viral vectors and the gene-editing reagents reduce the number of gene-modified stem cells for transplantation.[1,13–16] In addition, the committed progenitors are more susceptible to gene manipulation and compete with the HSCs during the gene manipulation process.[8] Soon after transplantation,

Correspondence: Dr. Saravanabhavan Thangavel, Centre for Stem Cell Research (CSCR), A Unit of InStem Bengaluru, Christian Medical College Campus, Vellore 632002, India. E-mail: sthangavel@cmcvellore.ac.in

DOI: 10.1089/hum.2021.089

gene-modified committed progenitor cells gradually diminish and only the gene-modified HSCs repopulate.[17] Thus, there is a significant decline in the frequency of gene-modified cells *in vivo*, rendering gene manipulation of committed progenitor cells less beneficial.

The insufficient quantity of gene-modified HSCs transplanted and retained *in vivo* demands the retrieval and manipulation of large doses of HSPCs from the patient, resulting in increased production cost.[17,18] For aforementioned reasons, effective genetic manipulation of $CD34^+CD133^+CD90^+$ enriched HSPCs could reduce the requirement for a large quantity of cells for manipulation and the need for high doses of gene manipulating reagents, thus simplifying the process and improving the efficacy.[18–21] In this study, we tested 11 small molecules that are known to expand umbilical cord blood (UCB)-HSPCs and identified a novel combination of small molecules which enriches the fraction of gene-modified $CD34^+CD133^+CD90^+$ HSCs in the mobilized peripheral blood (mPB) HSPC graft, resulting in an increased frequency of gene-modified cells *in vivo*.

METHODS

Purification of adult HSPCs

The leftover granulocyte colony-stimulating factor (GCSF)-mPB product after allogeneic stem cell transplantation was collected from the hematology department, Christian Medical College, Vellore, after IRB approval. $CD34^+$ cells were purified using CD34-positive selection kit (STEMCELL Technologies) and expanded with StemSpan SFEM II containing appropriate cytokines (stem cell factor [SCF] 240 ng/mL, FMS-like tyrosine kinase 3-ligand [Flt3-L] 240 ng/mL, thrombopoietin [TPO] 80 ng/mL, interleukin [IL]-6 40 ng/mL). The HSPCs were analyzed for cell surface markers, both after purification and on day 5 or 6 of the culture using BD Aria III Flow cytometer.

The study is approved by IRB and IBSC of Christian Medical College, Vellore, India.

Statistical analysis

Statistical analysis was performed using GraphPad Prism 8.0 (GraphPad Software). Error bars are presented as the mean ± SEM. Unpaired *t*-test values, number of independent replicates (*n*), and donors are indicated in the figure legend. *p* score of <0.05 is considered as statistically significant. Detailed description of methods and materials used in this study are depicted in Supplementary File.

RESULTS

Preferential expansion of HSCs results in culture enrichment of HSCs

The HSPC manipulation procedure for gene therapy requires up to 5 days of *ex vivo* culture.[4,10] To identify a culture condition that preserves the stemness of mPB-HSPCs during the 5-day culture, we cultured HSPCs in a stem cell culture media containing SCF, Flt3-L, TPO, and IL-6 cytokines and tested the supplementation of small molecules targeting chromatin modifiers (Trichostatin A, Nicotinamide, Resveratrol, and UM729), Wnt signaling (Prostaglandin E2), Notch signaling (3,5-difluorophen ylacetamide [DAPT]), p38-mitogen-activated protein kinases (SB203580), cell cycle (P18IN003), glucocorticoid receptor (Fluticasone), Aryl hydrocarbon receptor (SR1), and sphingolipid (4-hydroxyphenyl retinamide) that were previously shown to support UCB-HSPC expansion[22–32] (Fig. 1A).

Among the tested candidates, SR1, UM729, and Resveratrol showed significantly higher percentage of $CD34^+$ cells (Fig. 1B), and on testing these three compounds in different combinations, Resveratrol+UM729+SR1 (R+U+S/RUS) combination generated higher percentage of $CD34^+CD133^+$ cells compared to other treatment conditions (Fig. 1C and Supplementary Fig. S1A). On examination of the composition of the cell product, the RUS-treated HSPCs had an increased percentage of HSCs ($CD34^+CD133^+CD90^+$ cells) and decreased percentage of committed progenitors ($CD34^+CD133^-$ cells) and differentiated ($CD34^-$) cells than the individual compounds (Supplementary Fig. S2A). This suggests that RUS cocktail supplementation enrich the HSCs additively and thus provides an ideal *ex vivo* culture system for HSPCs.

To further strengthen the finding that HSCs are enriched on RUS treatment and to test whether HSC enrichment is associated with the proliferation or the maintenance of HSCs, we tested HSPCs from multiple healthy donors for their immunophenotype and proliferation rates. The RUS treatment consistently showed an increased percentage of HSCs, decreased committed progenitors, and differentiated cells over the vehicle. Of note, the proportion of HSCs, early progenitors and differentiated cells in RUS-treated cell products remained similar to that of uncultured HSPCs (day 0) (Fig. 1D and Supplementary Fig. S1B).

The growth kinetics and the carboxyfluorescein succinimidyl ester dye dilution analysis showed a slower proliferation of RUS-treated HSPCs (Supplementary Fig. S2B–D). Furthermore, the proliferation of total cells as well as the differentiated and committed progenitor cells was significantly reduced on RUS treatment. On the contrary, HSC proliferation was twofold higher suggesting preferential expansion of HSCs on RUS treatment (Fig. 1E and F). While committed progenitors are known to proliferate robustly compared to HSCs, the ratio of fold expansion was 1.2 (vs. 0.2 in control) and this phenomenon was specific to the RUS cocktail (Fig. 1G). The mean fluorescence intensity of CD34, CD133, and CD90 in the total cell population remained unaltered confirming that the changes are due to the increased number of HSCs (Supplementary Fig. S2E–G).

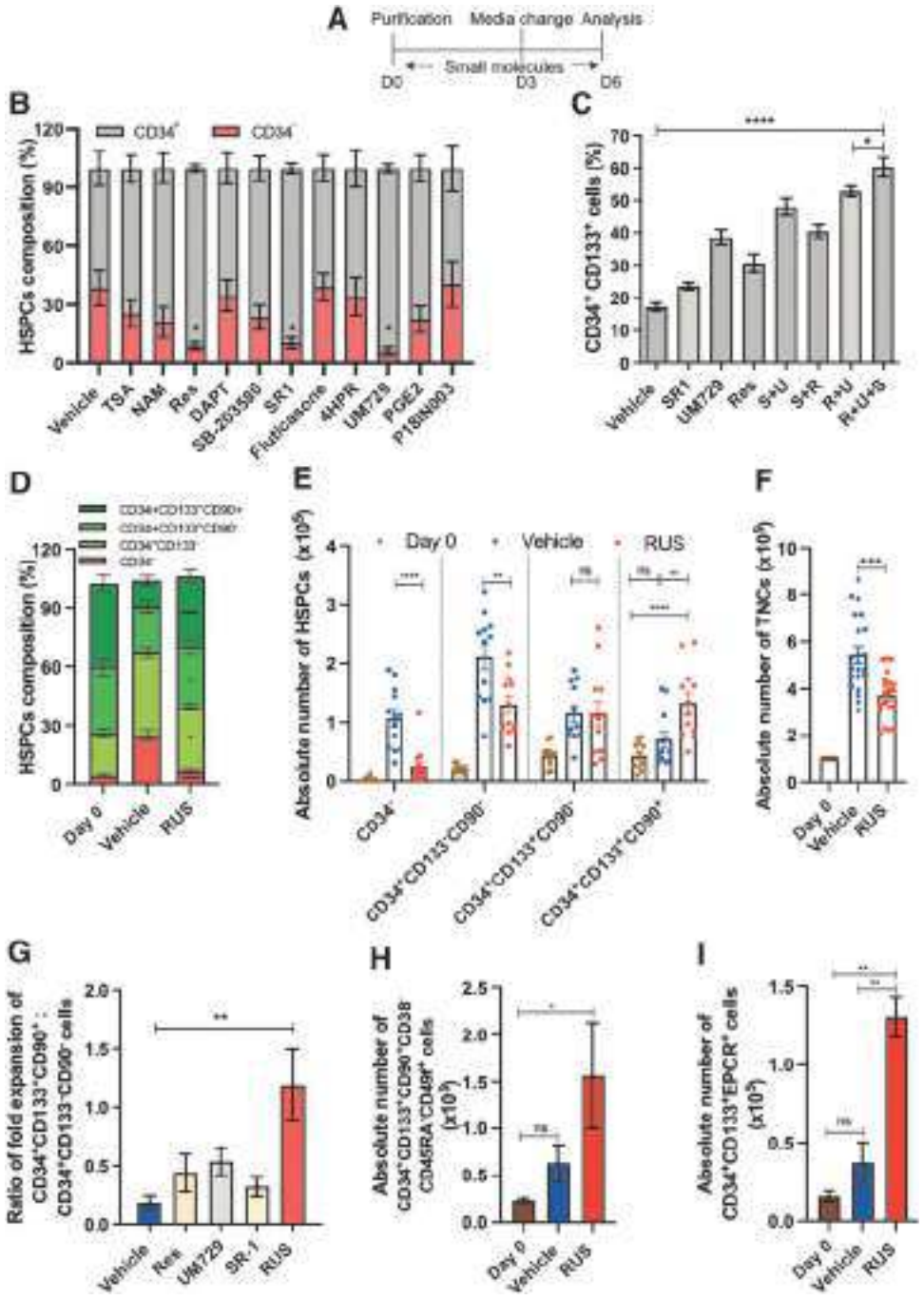

Figure 1. The RUS cocktail preferentially enriches the HSCs. **(A)** Experimental scheme: The mPB-HSPCs were cultured with the listed small molecules in the stem cell culture media containing cytokines for 5 days and analyzed by FACS for the markers for HSPCs. **(B)** Percentage of $CD34^+$ and $CD34^-$ cells. $n=6$, donors $=3$. **(C)** Percentage of cells positive for both CD34 and CD133. S+U = SR1+UM729, S+R = SR1+Resveratrol, R+U = Resveratrol+UM729, R+U+S = Resveratrol+UM729+SR1. $n=4$, donors $=2$. **(D)** The composition of subpopulations of HSPCs in day 0 (uncultured) and day 5 of the culture with vehicle (dimethylsulfoxide) or RUS (RUS = Resveratrol+UM729+SR1). The statistical comparison is between vehicle and RUS. $n=16$, donors $=7$. **(E)** Absolute number of subpopulations of HSPCs in day 0 and day 5 of the culture with vehicle or RUS. $n=12$, donors $=6$. **(F)** Absolute number of TNCs in day 0 and day 5 of culture with vehicle or RUS. $n=21$, donors $=7$. **(G)** Ratio of fold expansion of HSCs ($CD34^+CD133^+CD90^+$ cells) and committed progenitors ($CD34^+CD133^-CD90^-$ cells) in the HSPCs cultured with individual small molecules or the RUS cocktail. Fold expansions were calculated based on the increase in the absolute numbers from the input (day 0) numbers. $n=5$, donors $=2$. **(H)** Absolute number of $CD34^+CD133^+CD90^+CD38^-CD45RA^-CD49f^+$ HSCs in day 0 and day 5 of culture with vehicle or RUS. $n=6$, donors $=2$. **(I)** Absolute number of $CD34^+CD133^+EPCR^+$ HSCs after 5 days of culture. $n=3$, donors $=2$. Error bars represent mean ± SEM, ns. $^*p \le 0.05$, $^{**}p \le 0.01$, $^{***}p \le 0.001$, $^{****}p \le 0.0001$ (unpaired *t*-test, two-tailed). FACS, fluorescence-activated single cell sorting; HSC, hematopoietic stem cell; HSPC, hematopoietic stem and progenitor cell; mPB, mobilized peripheral blood; ns, nonsignificant; TNCs, total nucleated cells. Color images are available online.

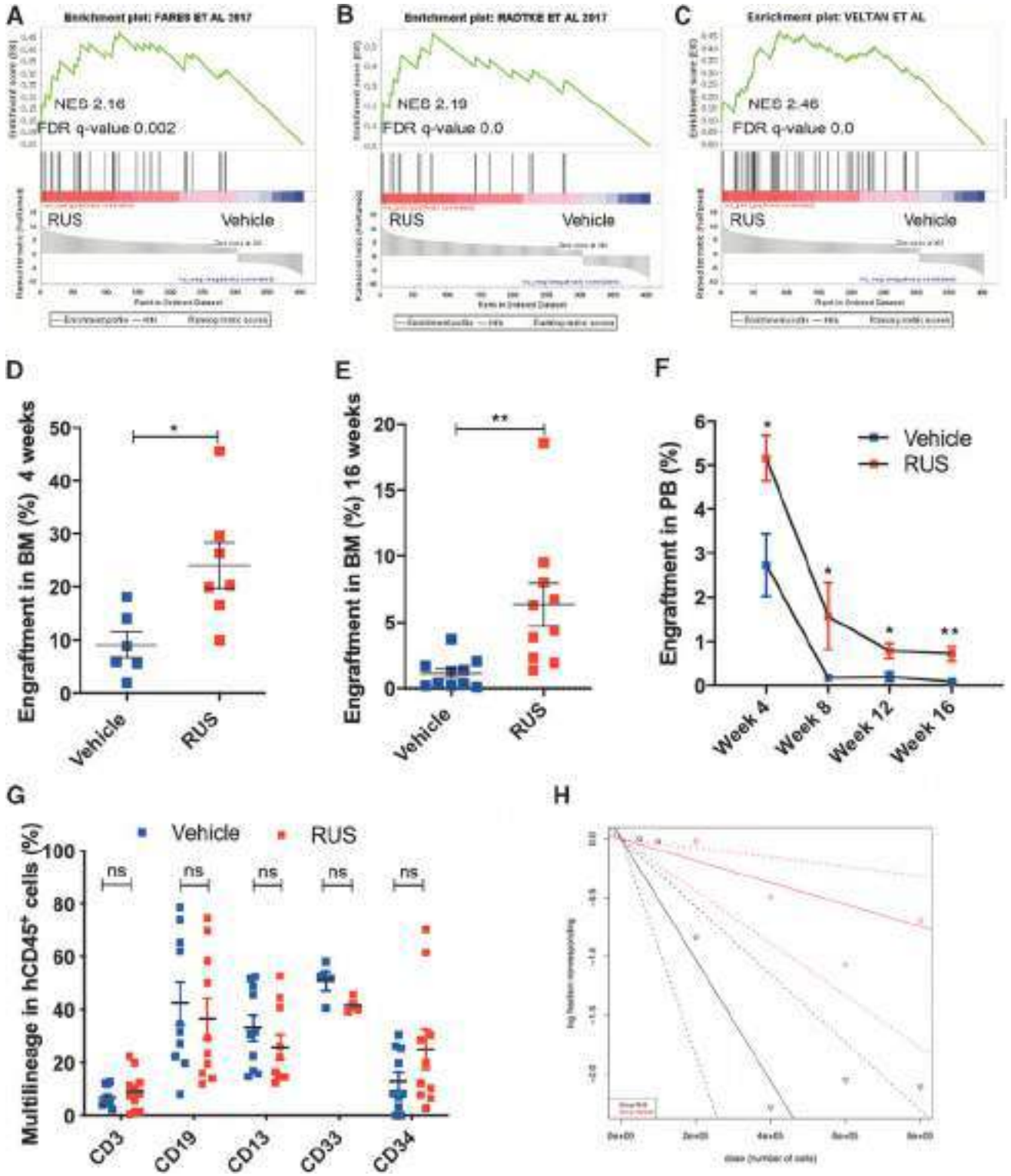

Figure 2. RUS-treated HSPCs showing gene sets of HSCs and enhanced engraftment *in vivo.* **(A)** GSEA of differentially expressed genes in HSPCs cultured for 5 days with vehicle or RUS. Gene list obtained from Fares *et al.*[34] NES = 2.16, $n = 4$, donors = 2. **(B)** GSEA of differentially expressed genes in HSPCs cultured for 5 days with vehicle or RUS. Gene list obtained from Radtke *et al.*,[37] NES = 2.19, $n = 4$, donors = 2. **(C)** GSEA of differentially expressed genes in HSPCs cultured for 5 days with vehicle or RUS. Gene list obtained from Velten *et al.*,[38] NES = 2.46, $n = 4$, donors = 2. **(D)** The mice were infused with HSPCs that were cultured for 5 days with vehicle or RUS. The human chimerism in the BM was analyzed 4 weeks post transplantation. Donors = 2. **(E)** The mice were infused with HSPCs that were cultured for 5 days with vehicle or RUS. The human chimerism in the mouse BM was analyzed 16 weeks posttransplantation. Donors = 3. **(F)** The human chimerism in mouse PB at different weeks postinfusion, $n = 4$. **(G)** The multilineage reconstitution of human cells in the mouse BM 16 weeks posttransplantation. Lymphoid cells (CD19 and CD3), myeloid cells (CD13 and CD33), and HSPCs (CD34). $n = 10$, donors = 3. **(H)** Limiting dilution analysis. The mice were infused with different doses (50,000, 100,000, 200,000, 400,000, 800,000) of HSPCs that were cultured for 5 days with vehicle or RUS. The human chimerism in the BM was analyzed 16 weeks posttransplantation. Long-term reconstitution frequency was estimated using the ELDA software.[62] Each *dot* depicts one mouse. Error bars represent mean ± SEM, ns. $*p \leq 0.05$, $**p \leq 0.01$ (unpaired *t*-test, two-tailed). BM, bone marrow; GSEA, gene set enrichment analysis; NES, normalized enrichment score; PB, peripheral blood. Color images are available online.

RUS treatment increased the absolute number and enriched the $CD34^+CD133^+CD90^+CD38^-CD45RA^-CD49f^+$ cells (Fig. 1H and Supplementary Figs. S1C and S2H) which is considered to be a stringent marker for the HSCs[33] and also $CD34^+CD133^+EPCR^+$ cells (Fig. 1I and Supplementary Fig. S2I), the marker for expanded HSCs.[34–36] These findings support the observation that RUS treatment enriches HSCs by inhibiting proliferation of differentiated and committed progenitor cells and preferentially allowing the proliferation of HSCs.

The dose reduction of RUS caused a decrease in the percentage of HSCs (Supplementary Fig. S3A), and its withdrawal resulted in the reduction of HSCs (Supplementary Fig. S3B), confirming that the effect is associated with the RUS treatment, and is reversible. RUS-mediated increase in HSCs was reproducible in different tested parameters, like with UM171, an analog of UM729[25] (Supplementary Fig. S3C), cytokine conditions (Supplementary Fig. S3D and E), stem cell culture media (Supplementary Fig. S3F), oxygen levels (Supplementary Fig. S3G), and cell culture plates (Supplementary Fig. S3H). Media change on day 3 (Supplementary Fig. S3I) and a low culture density ($\leq 2\times10^5$/mL) (Supplementary Fig. S3J) were found to promote HSC expansion on RUS treatment.

Culture-enriched HSCs resemble functional HSCs in gene sets and stemness characteristics

Gene expression analysis showed that 305 genes were upregulated, and 100 genes were downregulated on RUS treatment (Supplementary Fig. S4A–C). The gene set enrichment analysis (GSEA) with the gene lists for the *in vivo* repopulating HSCs[34,37,38] showed a significantly high normalized enrichment score (NES) (Fig. 2A–C), confirming the upregulation of stem cell signatures. KEGG2019 pathway analysis showed an upregulation of genes associated with cell adhesion (Supplementary Fig. S4D), which is crucial for long-term engraftment[39] and a downregulation of heme metabolism, janus kinase/signal transducers and activators of transcription - 3 (JAK/STAT3) pathway involved in cell division, and transforming growth factor-β-signaling pathways (Supplementary Fig. S4E) that are associated with robust proliferation and exhaustion of HSCs.[40,41]

The RUS-treated HSPCs retained their differentiation potential in the colony formation assay (Supplementary Fig. S5A) and differentiated into megakaryocytes, macrophages, and erythroid cells in suspension culture (Supplementary Fig. S5B–D). In addition, they showed twofold increase in transwell migration in response to stromal cell-derived factor (SDF)-1α stimuli (Supplementary Fig. S5E), twofold decrease in the reactive oxygen species (ROS) levels (Supplementary Fig. S5F), and an increase in the live cells when cultured for 12 days (Supplementary Fig. S5G). The differentiation potential, SDF-1α response, reduced ROS,[42] and apoptosis indicates that the RUS-treated cells retain the stem cell characteristics *in vitro*.

HSCs-enriched graft exhibits enhanced engraftment and repopulation *in vivo*

To evaluate whether RUS treatment preserves functional HSCs, we cultured HSPCs for 5 days and transplanted into irradiated NSG mice. The early phase of HSPC engraftment is critical for gene therapy and the RUS group showed a 2.6-fold higher bone marrow (BM) engraftment of $hCD45^+$ cells, 4 weeks posttransplantation (Fig. 2D), suggesting rapid engraftment. Similarly, the RUS group showed a 5.6-fold increase in the long-term engraftment (16 weeks posttransplantation) (Fig. 2E). Peripheral blood (PB) chimerism analysis also showed early and persistent engraftment (Fig. 2F).

All animals of RUS group showed PB engraftment till 16 weeks of infusion (vs. 16.6% in control) (Supplementary Table S1) and retained multilineage repopulation potential, forming human T-lymphoid, B-lymphoid, and myeloid cells with no bias toward specific lineage (Fig. 2G). The limiting dilution analysis indicated 1 in 193,826 RUS-treated cells as long-term-HSCs (vs. 1/1074091 in vehicle), confirming a sixfold increase in stem cell frequency (Fig. 2H). All these data indicate that RUS-treated graft consists of increased number of functional HSCs compared to the graft maintained in regular culture conditions.

Figure 3. RUS treatment enriches the HSCs in patient HSPCs and supports the culture of sort enriched HSCs. **(A)** Absolute number of subpopulations of HSPCs from SCD patient, in day 0 and day 5 of culture with vehicle or RUS. $n=1$. **(B)** Absolute number of subpopulations of HSPCs from β-thalassemia patient, in day 0 and day 5 of culture with vehicle or RUS. $n=1$. **(C)** Absolute number of subpopulations of HSPCs from hemophilia patient, in day 0 and day 5 of culture with vehicle or RUS. $n=2$. **(D)** Number of GEMM colonies obtained in MethoCult analysis after seeding 500 SCD-HSPCs that are cultured with vehicle or RUS for 5 days $n=3$. **(E)** Transwell migration assay; percentage of SCD-HSPCs responded to SDF-1α in the lower chamber. The HSPCs were cultured with vehicle or RUS for 5 days before the assay. $n=2$. **(F)** Transwell migration assay; percentage of β-thalassemia-HSPCs responded to SDF-1α in the lower chamber. The HSPCs were cultured with vehicle or RUS for 5 days before the assay. $n=4$. **(G)** Composition of subpopulations of HSPCs. The unsorted and $CD34^+CD90^+$ sorted cells were cultured with vehicle or RUS for 5 days. The $CD34^+CD90^+$ sorting was performed on day 0 and immediately seeded for culture. $n=3$, donors = 2. **(H)** FACS analysis of $CD34^+CD90^+$ cells in the unsorted and $CD34^+CD90^+$-sorted cells that are cultured for 5 days with vehicle or RUS. $n=3$, donors = 2. **(I)** Number of GEMM colonies obtained in MethoCult analysis after seeding unsorted and $CD34^+CD90^+$-sorted HSPCs that are cultured for 5 days with vehicle or RUS. $n=3$, donors = 2. **(J)** FACS analysis of $CD34^+CD90^+$ cells in the $CD34^+CD90^-$-sorted cells that are cultured for 12 and 120 h. $n=3$, donors = 2. **(K)** Absolute number of TNCs in $CD34^+CD90^-$-sorted HSPCs after 5 days of culture with vehicle or RUS. $n=3$, donors = 2. Error bars represent mean ± SEM, ns. $^*p\leq0.05$, $^{**}p\leq0.01$ (unpaired *t*-test, two-tailed). GEMM, granulocyte, erythrocyte, monocyte, megakaryocyte; SCD, sickle cell disease; SDF, stromal cell-derived factor. Color images are available online.

HSC culture enrichment is independent of mobilization regimens and disease characteristics

The patient HSPCs are the target cells for gene manipulation in the HSPC gene therapy. To understand whether different mobilization regimens and disease characteristics influence the culture enrichment of HSCs, we first tested the effect of RUS treatment in plerixafor mPB-HSPCs from a sickle cell disease (SCD) patient. The composition of HSPCs in SCD patient was observed to be different from

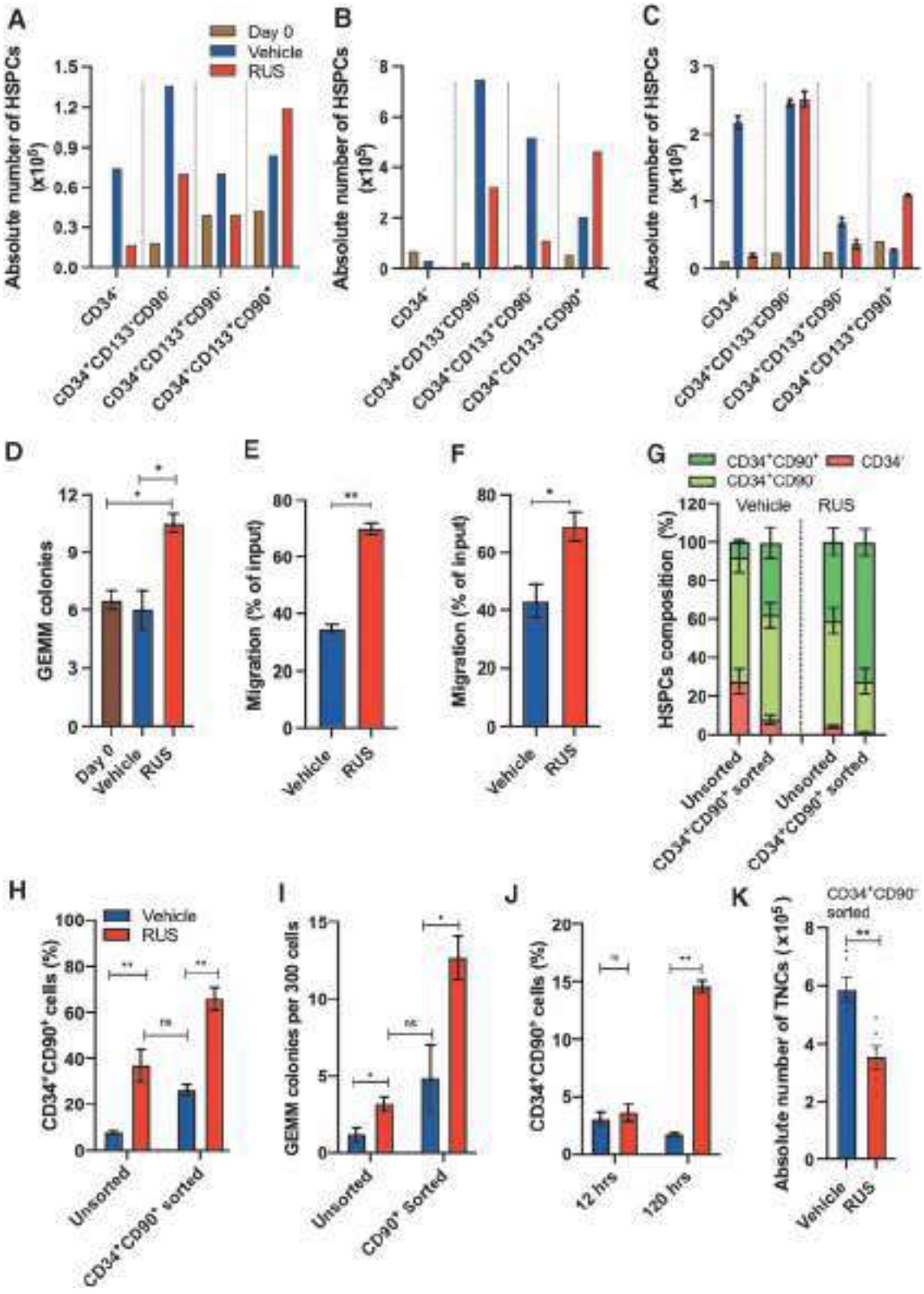

healthy individuals.[43] However, consistent with the GCSF mobilized healthy donor cells, RUS treatment inhibited the proliferation of differentiated and committed progenitor cells and supported the proliferation of the HSCs (Fig. 3A). The HSPCs of the β-thalassemia patient that are derived from the stressed BM microenvironment responded to the RUS treatment with an increase in the absolute number of HSCs by twofold (Fig. 3B).

In line with this, the GCSF mPB-HSPCs from a hemophilia patient also showed an increase in the absolute numbers of HSCs (Fig. 3C). The RUS treatment generated a high frequency of granulocyte, erythrocyte, monocyte, megakaryocyte (GEMM) colonies (Fig. 3D), the most primitive progenitor colonies in the colony forming unit (CFU) assay and improved the transwell migration potential of both the SCD and β-thalassemia patient HSPCs (Fig. 3E, F). All these observations support the application of RUS treatment for HSPC gene therapy.

Culture enrichment procedure supports the sort enriched HSCs

The existing approach for HSC enrichment is the fluorescence-activated single cell sorting based sort purification of $CD34^+CD90^+$ cells followed by culturing, to execute the gene manipulation.[21] We compared the HSC yield obtained on day 5 by sort enrichment and culture enrichment. The sort enriched $CD34^+CD90^+$ HSCs, reduced in their frequency on culture, and the frequency was similar to the HSCs found in the unsorted HSPCs cultured with RUS (Fig. 3G, H and Supplementary Fig. S6A). This effect was also mirrored in the CFU analysis (Fig. 3I). On combining, that is, culturing the sort-enriched $CD34^+CD90^+$ cells with RUS, a higher frequency of HSCs and GEMM colonies were generated (Fig. 3G–I). All these assays suggest the benefit of supplementing RUS for the culture of both the unsorted and sorted cells.

The sorted $CD34^+CD90^-$ cells had a basal frequency of $CD34^+CD90^+$ cells after 12 h of culture with vehicle or RUS. This rules out any treatment mediated conversion of $CD34^+CD90^-$ cells into $CD34^+CD90^+$ cells.[44] On further analysis, after 120 h, RUS-treated cells showed an increase in the percentage of $CD34^+CD90^+$ cells from 4% to 15%, with a twofold reduction in the proliferation of total cells (Fig. 3J, K). This strengthens the observation of preferential proliferation and enrichment of HSCs with RUS treatment.

Culture enrichment of HSCs increases the frequency of transduced HSCs

As the HSCs resist gene manipulation,[8,45] increasing the HSC population alone will not be beneficial unless these cells are amenable for gene manipulation. To test whether culture enriched HSCs can be manipulated, we transduced the HSPCs with a lenti-green fluorescent protein (GFP) vector and observed that RUS treatment retained the HSC enrichment even after the transduction stress (Fig. 4A and Supplementary Fig. S7A), unaltered overall transduction efficiency (Supplementary Fig. S7B), generated a 4.2-fold increase in the frequency and in the absolute number of $GFP^+CD34^+CD90^+$ HSCs (Fig. 4B and Supplementary Fig. S7C), and had the ratio of GFP^+HSCs to GFP^+ progenitors as 2.9 (vs. 0.4 in control) (Fig. 4C).

The RUS-treated SCD-HSPCs also showed a high frequency and the absolute number of GFP^+HSCs and reduced frequency and absolute number of GFP^+ progenitors over the control (Fig. 4D and Supplementary Fig. S7E and F). Similar results were obtained with the healthy donor HSPCs that were cultured for 5 days (Supplementary Fig. S8A–E).

The ratio of transduction between the $CD34^+CD90^+$ fraction and $CD34^+CD90^-$ fraction in RUS-treated cells was 1.1 (vs. 0.8 in control), suggesting the equal transduction in HSCs and progenitors (Supplementary Fig. S8D). Thus, the availability of more HSCs has resulted in the increase in the frequency of GFP^+HSCs. This observation was further supported by varying degree of HSC enrichment by individual small molecules and proportional increase in of GFP^+HSCs (Fig. 4E).

To test whether RUS treatment primes the HSC fraction for transduction, cultured HSPCs were sort-purified for $CD34^+CD90^+$ HSCs and transduced. The RUS treatment showed a higher frequency of GFP^+HSCs (Fig. 4F) and transduction in HSCs (Fig. 4G and Supplementary Figs. S6B, S7D and S8E). This suggests that the HSC fraction of RUS is more responsive to transduction than that of vehicle.

The RUS-cultured HSPCs and the sorted HSCs had a similar percentage of GFP^+HSCs, indicating that the treatment generates gene-modified HSCs at a frequency similar to the protocol that involves sort purification and transduction. Culturing the sorted HSCs with RUS further improved the yield of GFP^+HSCs. RUS treatment also produced fourfold more GFP^+HSCs than the best-known transduction enhancer Cyclosporin H (CsH).[46] Combining both had a little effect on the GFP^+HSCs but increased the overall percentage of GFP^+ cells (Fig. 4H, I and Supplementary Fig. S6C).

Collectively, the RUS-treated cell product contains a higher frequency of gene-modified HSCs compared to control and this fraction of gene-modified HSCs occupy an equal or a greater portion in the RUS-treated cell product than the gene-modified progenitors. This effect is distinct from conventional gene therapy products that have greater number of gene-modified progenitors.[1]

Culture enrichment of HSCs increases the frequency of gene-edited HSCs

To investigate the impact of culture enrichment of HSCs on gene editing, we gene-edited three different loci

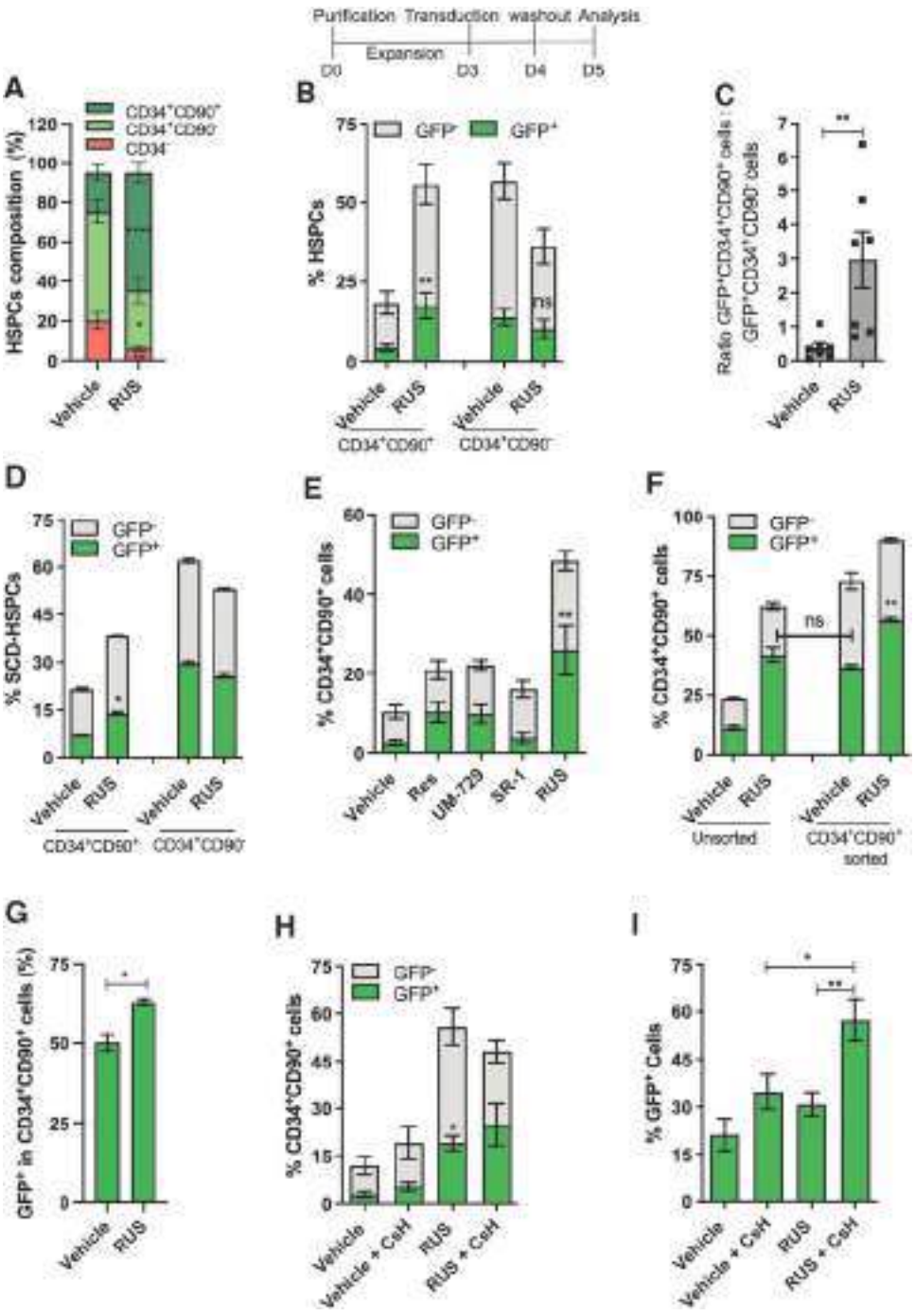

Figure 4. The RUS treatment increases the frequency of lentiviral transduced $CD34^+CD90^+$ HSCs. *Top*: Scheme of the experiment. Vehicle and RUS-treated HSPCs were transduced with Lenti-GFP vector on day 3 and analyzed by FACS 48 h posttransduction. The treatment was maintained throughout the culture period. Results are presented as mean ± SEM, ns. $*p \le 0.05$, $**p \le 0.01$, $****p \le 0.0001$ (unpaired *t*-test, two-tailed), $n = 8$, donors = 3. **(A)** Percentage of HSPC subpopulations 48 h posttransduction. **(B)** Percentage of GFP^+ and GFP^- cells in the $CD34^+CD90^+$ and $CD34^+CD90^-$ subpopulations. **(C)** The ratio of $GFP^+CD34^+CD90^+$:$GFP^+CD34^+CD90^-$ cells. **(D)** Percentage of GFP^+ and GFP^- cells in the $CD34^+CD90^+$ and $CD34^+CD90^-$ subpopulations of SCD-HSPCs. **(E)** Percentage of $GFP^+CD34^+CD90^+$ and $GFP^-CD34^+CD90^+$cells in the HSPCs that were treated with individual small molecules or with the RUS cocktail. **(F)** Percentage of $GFP^+CD34^+CD90^+$ and $GFP^-CD34^+CD90^+$cells. The HSPCs were cultured with vehicle or RUS for 3 days and sorted for $CD34^+CD90^+$ cells. The unsorted and sorted cells were transduced with Lenti-GFP virus and analyzed 48 h posttransduction. Posttransduction, the medium was not supplemented with RUS. $n = 2$, donor = 1. **(G)** Percentage of transduction in $CD34^+CD90^+$ cells. The data were analyzed from Fig. 4F. **(H)** Percentage of $GFP^+CD34^+CD90^+$ and $GFP^-CD34^+CD90^+$ cells. HSPCs were cultured with vehicle or RUS and treated with or without CsH, transduced with Lenti-GFP and analyzed 48 h posttransduction. The RUS was maintained posttransduction. $n = 6$ (donors = 2) **(I)**. Percentage of total GFP^+ cells from experiment **(H)**. CsH, cyclosporin H; GFP, green fluorescent protein. Color images are available online.

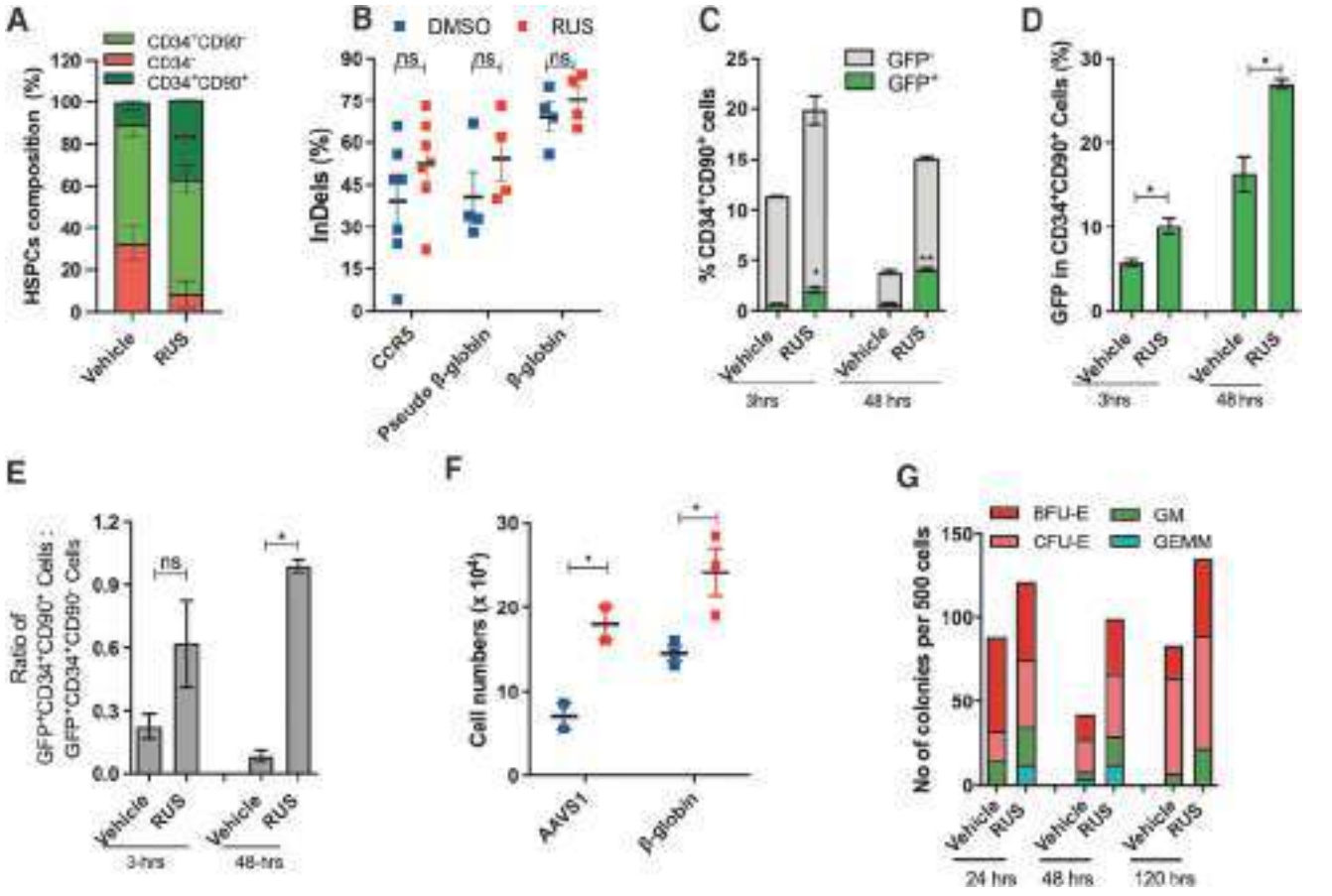

Figure 5. The RUS treatment increases the frequency of gene-edited $CD34^+CD90^+$ HSCs. **(A)** HSPCs were cultured for 3 days with vehicle or RUS and edited with Cas9-RNP. The edited cells were collected 72 h postediting. Percentage of HSPC subpopulations postelectroporation. RUS treatment was maintained throughout the culture period. $n=2$, donors = 2. **(B)** Percentage of InDels. Each *dot* depicts individual experiments. The regions targeted by Cas9-RNP are indicated in *x*-axis. **(C)** Percentage of $GFP^+CD34^+CD90^+$ and $GFP^-CD34^+CD90^+$ cells; HSPCs were cultured for 3 days and edited with Cas9-GFP RNP targeting pseudo β-globin locus. The $CD34^+CD90^+$ fraction was analyzed for GFP 3 and 48 h postelectroporation. $n=2$, donors = 1. **(D)** The percentage of GFP within $CD34^+CD90^+$ fraction. **(E)** The ratio of $GFP^+CD34^+CD90^+$:$GFP^+CD34^+CD90^-$ cells in the HSPCs that were cultured with vehicle or RUS. **(F)** HSPCs were cultured for 3 days and edited with Cas9-RNP targeting AAVS1 and β-globin loci. The cell numbers were calculated 72 h postediting using trypan blue dye exclusion. Donors = 2. **(G)** MethoCult analysis of HSPCs, edited at different timepoints of culture (24, 48, 120 h) and plated 48 h postelectroporation. $n=1$. Results are presented as mean ± SEM, ns.*$p \le 0.05$, **$p \le 0.01$, ***$p \le 0.001$ (unpaired *t*-test, two-tailed). RNP, ribonucleoprotein. Color images are available online.

with Cas9 ribonuleoprotein (RNP) and observed that the RUS treatment retained the HSC enrichment even after the electroporation stress (Fig. 5A), modestly improved indel rates with 72 h of treatment (pre- and postediting) (Fig. 5B and Supplementary Fig. S9A) and showed no alterations in the pattern of indels (Supplementary Fig. S9B).

To test the gene editing in the HSC fraction of HSPCs, we edited with Cas9-GFP RNP, which showed a threefold increase in the frequency of GFP^+HSCs in the RUS-treated cells at 3 h postelectroporation, which doubled in 48 h (Fig. 5C) pointing that the initial increase in GFP^+ HSCs is further boosted by preferential proliferation of HSCs. The HSC fraction of RUS-treated cells had twofold more GFP suggesting that the HSC fraction is more permissive for editing compared to the HSC fraction of vehicle (Fig. 5D). These observations were consistent in the HSPCs that were cultured for 5 days before nucleofection with different doses of Cas9-GFP RNP (Supplementary Fig. S9C, D). The ratio analysis of GFP^+HSCs and GFP^+ progenitors showed that the RUS-treated cell product had an equal proportion of gene-edited HSCs and progenitors after 48 h of culture, whereas the vehicle had more gene-edited progenitor cells (Fig. 5E). In addition, RUS-treated cells recovered well from electroporation stress (Fig. 5F) and generated a higher number of CFU counts in all the tested time points (Fig. 5G).

Collectively, higher frequency of HSCs (available during gene editing), their enhanced permissiveness for gene-editing, improved viability, and preferential proliferation of HSCs (post-gene editing) contribute to the increased frequency of gene-edited HSCs.

Culture enrichment increases the frequency of gene-modified cells *in vivo*

Supplementing RUS to the HSPC culture generated an increased frequency of gene-modified HSCs *in vitro*. To

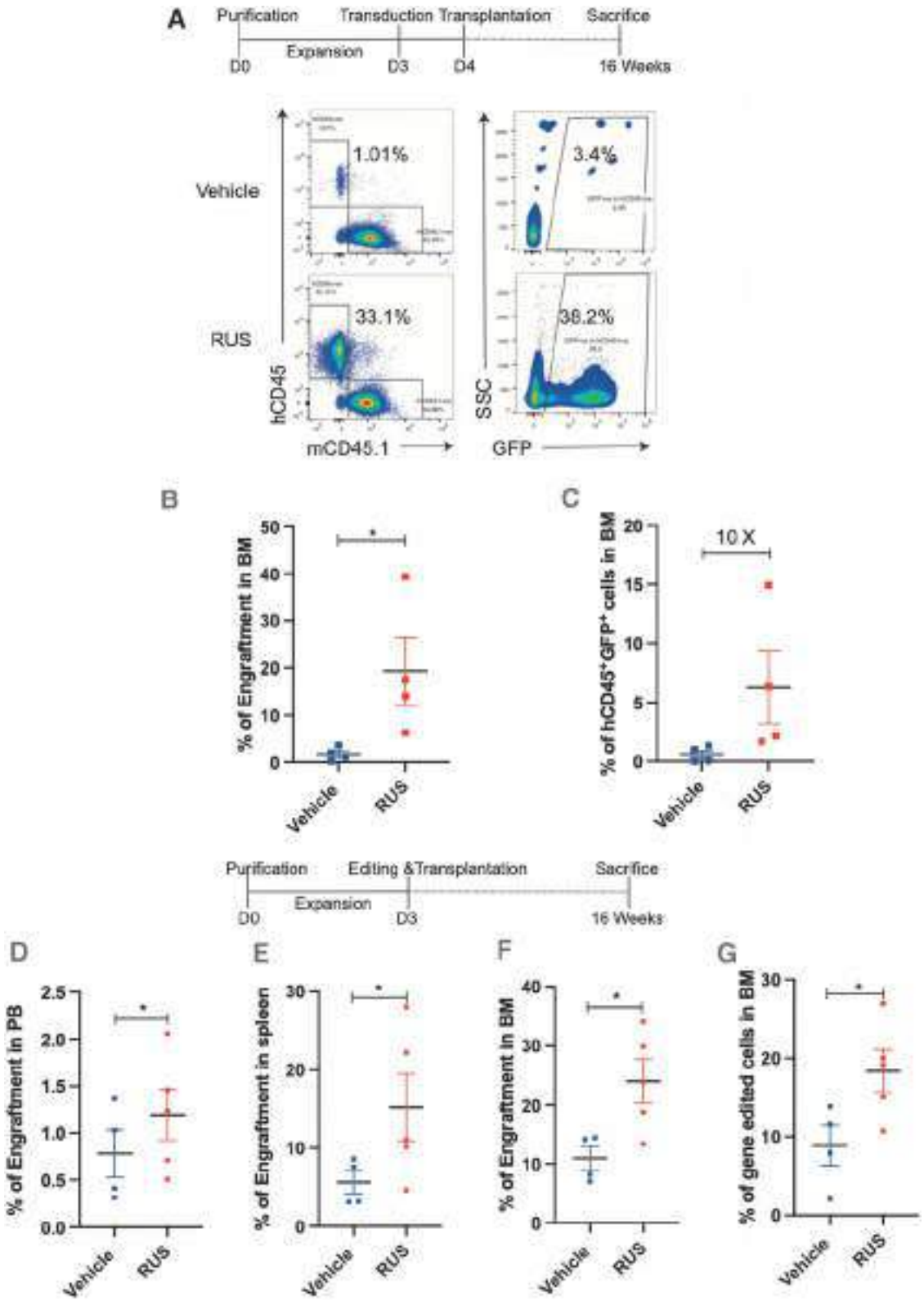

Figure 6. The RUS treatment increases the frequency of gene modified cells *in vivo*. *Top*: The outline of the experimental scheme. HSPCs were cultured for 3 days with vehicle or RUS and transduced with Lenti-GFP vector at multiplicity of infection 40 on day 3 and transplanted on day 4. The animals were sacrificed on 16 weeks posttransplantation for mice BM analysis. Error bars represent mean ± SEM, ns. $*p \leq 0.05$ (unpaired *t*-test, two-tailed). **(A)** Representative FACS plot showing the $hCD45^{+}GFP^{+}$ cells in the mouse BM. The *inset* refers to human cells (*left*) and GFP percentage in human cells (*right*). **(B)** The engraftment of human cells in mouse BM at 16 weeks post infusion. $n=4$. **(C)** The gene-modified human cell ($hCD45^{+}GFP^{+}$ cells) chimerism in mouse BM at 16 weeks postinfusion. $n=4$. **(D)**.*Top*: experimental scheme. The HSPCs were cultured for 3 days, gene edited with CCR5 targeting sgRNA on day 3 and transplanted immediately postelectroporation. The animals were sacrificed at 16 weeks for mice BM analysis. *Bottom*: The engraftment of human cells in mouse PB at 16 weeks postinfusion (mean ± SEM, $n=4$). **(E)** The human cells engraftment in mouse spleen at 16 weeks postinfusion. **(F)** The engraftment of human cells in mouse BM at 16 weeks postinfusion. **(G)** The human gene-modified cell (hCD45+gene-edited cells) chimerism in mouse BM at 16 weeks postinfusion. Color images are available online.

know whether this advantage is retained *in vivo*, the HSPCs were transduced with the Lenti-GFP vector on day 3 of the culture and infused into NSG mice on day 4 (Supplementary Fig. S10A, B). The RUS-cultured cells displayed up to 11-fold increased human cell engraftment in the mouse BM at 16 weeks posttransplantation (Fig. 6A, B). The frequency of GFP^+ human cells were also up to 10-fold higher in the BM (Fig. 6C and Supplementary Fig. S10C–G). While no mice showed PB engraftment of gene-modified cells in the control, 50% of mice had PB engraftment in RUS-treated group (Supplementary Fig. S10E), confirming that the RUS treatment enhances the generation of functional gene-modified cells.

The experimental scheme for transplantation of gene-edited cells was specifically designed to negate the positive effects of RUS on the preferential proliferation of HSCs post-gene editing, thus focusing on the availability and amenability of HSC fraction for editing.

The vehicle and RUS-treated HSPCs were gene-edited for the CCR5 locus on day 3 and transplanted immediately postelectroporation. Sixteen weeks posttransplantation, there was 1.5-, 2.2-, and 2.7-fold increase in the engraftment, respectively, in PB, spleen, and BM (Fig. 6D–F). Sanger-sequencing and Inference of CRISPR Edits analysis of BM cells revealed a twofold increase in the frequency of CCR5 gene-edited human cells (Fig. 6G). This confirms that the RUS-mediated improved HSC frequency and permissiveness (pre-gene editing *in vitro*) resulted in an increase in the frequency of gene-edited cells *in vivo*. Culturing the cells with RUS post-gene editing will allow the preferential proliferation, further improving the frequency of gene-edited cells *in vivo.*

DISCUSSION

Accelerated engraftment and high frequency of gene-modified cells *in vivo* are crucial for the success of the HSPC gene therapy.[47,48] In this regard, we have developed a refined culture system for the HSPCs and made the following important observations; *ex vivo* culture of mPB-HSPCs with the small molecule cocktail RUS strongly restricts the proliferation of differentiated and progenitor cells and preferentially allows the proliferation of HSCs, resulting in enriched HSCs in the cultured graft and robust engraftment *in vivo*. These HSCs are permissive for gene manipulation at an enhanced frequency. The preferential expansion of HSCs and their enhanced gene manipulation increases the frequency of *in vivo* repopulating gene-modified cells up to 10-fold.

In contrast to the strategies applied for expanding UCB-HSPCs, which necessitate several hundred-fold expansions for clinical utility, a single BM harvest can provide sufficient number of cells for manipulation, thus a robust total cell expansion is not crucial for adult HSPCs. Instead, the harvested cells should retain the engraftment potential after *ex vivo* culture and gene manipulation. The *in vivo* clonal tracking of lentiviral integration sites demonstrated that the gene-modified cells in transplanted patients are derived from 2,000–50,000 gene-modified HSC clones, despite the infusion of a minimum 6×10^6 cells/kg of patient.[49,50]

Studies have documented that poor engraftment of *ex vivo* cultured HSPCs is due to disruption of adhesion molecules.[16,51,52] The upregulation of adhesion molecules in RUS-treated cells and the enhanced engraftment in the NSG mice demonstrate that the adhesion properties are preserved in RUS-treated cells, thus mediating long-term engraftment *in vivo*. The individual small molecules of our cocktail expand both the progenitor and HSC population. However, the cocktail usage preferentially expands the HSCs over the progenitors or the differentiated cells. SR1, UM171/729, and Resveratrol increases the UCB-HSPC numbers by inhibiting aryl hydrocarbon receptor, Lysine-specific demethylase 1A, and regulating cell cycle, respectively.[24,25,53,54] These findings suggest that different pathways are being targeted, and the synergized effect of the RUS works in nonoverlapping pathways to inhibit the proliferation of differentiated and progenitor cells during expansion.

Phase I/II clinical trials with SR1 and UM171 have shown that the small molecule expanded UCB-HSPCs engrafted and reconstituted the blood stream with no adverse events[55,56] supporting their application in culturing adult HSPCs. A recent study has shown that on sphingolipid modulation, autophagy is activated in the HSCs, but not in the progenitors, restricting the proliferation of progenitors in the *ex vivo* culture.[32] This supports the notion that the progenitor cells and HSCs respond differentially to culture conditions. The mobilization regimes such as GCSF and plerixafor were shown to mobilize different subpopulations of HSPCs[57,58] and the disease characteristics were also shown to alter the composition of HSPCs.[43] Despite these variations, we consistently observed a culture enrichment of HSCs by RUS treatment strengthening its usage in the HSPC gene therapy.

The mechanism by which RUS makes HSC fraction more responsive for gene manipulation is yet to be deciphered. Few small molecules such as CsH reduce the innate immune response during the transduction process, thus enhancing the viral transduction.[46,59] Supplementing CsH with RUS has not additively increased the frequency of GFP^+ HSCs (Fig. 4H and I). Also, Caraphenol A, a resveratrol trimer, was shown to increase the transduction by suppressing the innate immune response of the HSPCs.[59] The RUS-treated HSPCs show significant downregulation of JAK STAT3 signaling, which mediates the immune response (Fig. S4E). All these suggest that RUS treatment may have partly reduced the activation of the immune response pathway to make HSCs more permissive to genetic manipulation.

UM171, also have been reported to improve the viral transduction in HSPCs.[60] Similar to HSC enrichment, we observe an additive effect in the increase of gene manipulated HSCs, upon the cocktail usage. Recent reports linked the gene-editing stress with viability of cells.[61] RUS-treated cells have downregulation of apoptosis pathway, less ROS levels and apoptosis (Supplementary Fig. S5F, G). This could be a potential reason for increased viability in these cells post-gene editing.

Currently, there are efforts to sort the HSCs for gene manipulation procedures.[17,18,21] These protocols first sort the immunophenotypic HSCs, manipulate them in *ex vivo* culture, and infuse them along with the nonmanipulated progenitor cells to support immediate granulopoiesis after the transplantation. The RUS treatment-mediated enrichment approach is devoid of flow sorting, and the RUS-treated cell products also have gene modified progenitor cells at a lesser frequency. Thus, with this approach, the need for ''add-back'' of progenitor cells is not required. Interestingly, the yield of gene modified HSCs on RUS treatment matches to the yield obtained by the sorting procedure (Fig. 3H and 4F). The combination of sort-purification and culture enrichment approaches described (Fig. 4F) could be a potential way forward to reap the benefits of both the sort-purification and culture enrichment approaches.

CONCLUSIONS

Culturing HSPCs with the identified small molecule cocktail of Resveratrol, UM729, and SR1 significantly enhances the generation of gene-modified HSCs, a key step in HSPC gene therapy. The high frequency of gene-modified cells is achieved by the preferential proliferation of HSCs and by the enhanced susceptibility of HSCs for gene modification. This procedure should reduce the doses of HSPCs required for gene manipulation and also the usage of viral vectors and gene editing reagents without compromising the rapid and long-term engraftment potential. This will decrease the manufacturing cost of the gene-modified cells and increase the accessibility to HSPC gene therapy.

AUTHORS' CONTRIBUTIONS

Collection and/or assembly of data, data analysis, and interpretation, A.C.C., V.V, K.V.K., S.S., P.B., M.K.K.A., K.C., A.B., N.S.R, and V.R.; administrative support, S.K. and S.K.M.; provision of study material, A.S., S.R.V, and K.M.M; conception and design, financial support, data analysis and interpretation, article writing, and final approval of article, S.T.

ACKNOWLEDGMENTS

The authors thank Dr. Somadutta Dhir for her help in analyzing GSEA; Dr. Sandya Rani for her help with flow cytometry sample acquisition; Dr. Vigneshwar for maintaining the NSG mice.

AUTHOR DISCLOSURE

No competing financial interests exist.

FUNDING INFORMATION

This work was funded by the Department of Biotechnology, Government of India (grant no. BT/PR26901/MED/31/377/2017). A.C.C. is funded by an ICMR-SRF fellowship (2019-4018/SCR-BMS). K.V.K is funded by a DST-INSPIRE fellowship (IF180018), S.S. by a DBT-JRF fellowship, and P.B by a CSIR-JRF fellowship.

SUPPLEMENTARY MATERIAL

Supplementary File
Supplementary Table S1
Supplementary Figure S1
Supplementary Figure S2
Supplementary Figure S3
Supplementary Figure S4
Supplementary Figure S5
Supplementary Figure S6
Supplementary Figure S7
Supplementary Figure S8
Supplementary Figure S9
Supplementary Figure S10

REFERENCES

1. Naldini L. Genetic engineering of hematopoiesis: current stage of clinical translation and future perspectives. EMBO Mol Med;11:e9958.
2. Thompson AA, Walters MC, Kwiatkowski J, et al. Gene therapy in patients with transfusion-dependent β-thalassemia. N Engl J Med 2018;378:1479–1493.
3. Ribeil J-A, Hacein-Bey-Abina S, Payen E, et al. Gene therapy in a patient with sickle cell disease. N Engl J Med 2017;376:848–855.
4. Ferrua F, Cicalese MP, Galimberti S, et al. Lentiviral haemopoietic stem/progenitor cell gene therapy for treatment of Wiskott-Aldrich syndrome: interim results of a non-randomised, open-label, phase 1/2 clinical study. Lancet Haematol 2019;6:e239–e253.
5. Staal FJT, Aiuti A, Cavazzana M. Autologous stem-cell-based gene therapy for inherited disorders: state of the art and perspectives. Front Pediatr 2019;7:443.

6. Frangoul H, Altshuler D, Cappellini MD, et al. CRISPR-Cas9 gene editing for sickle cell disease and β-thalassemia. N Engl J Med 2021;384:252–260.
7. Xu L, Wang J, Liu Y, et al. CRISPR-edited stem cells in a patient with HIV and acute lymphocytic leukemia. N Engl J Med 2019;381:1240–1247.
8. Genovese P, Schiroli G, Escobar G, et al. Targeted genome editing in human repopulating haematopoietic stem cells. Nature 2014;510:235–240.
9. Morris EC, Fox T, Chakraverty R, et al. Gene therapy for Wiskott-Aldrich syndrome in a severely affected adult. Blood 2017;130:1327–1335.
10. Kohn DB, Booth C, Kang EM, et al. Lentiviral gene therapy for X-linked chronic granulomatous disease. Nat Med 2020;26:200–206.
11. Aiuti A, Biasco L, Scaramuzza S, et al. Lentiviral hematopoietic stem cell gene therapy in patients with wiskott-Aldrich syndrome. Science 2013;341: 1233151.
12. Gomez-Ospina N, Scharenberg SG, Mostrel N, et al. Human genome-edited hematopoietic stem cells phenotypically correct Mucopolysaccharidosis type I. Nat Commun 2019;10:4045.
13. Grez M, Reichenbach J, Schwäble J, et al. Gene therapy of chronic granulomatous disease: the engraftment dilemma. Mol Ther 2011;19:28–35.
14. Mazurier F, Gan OI, McKenzie JL, et al. Lentivector-mediated clonal tracking reveals intrinsic heterogeneity in the human hematopoietic stem cell compartment and culture-induced stem cell impairment. Blood 2004;103:545–552.
15. Piras F, Riba M, Petrillo C, et al. Lentiviral vectors escape innate sensing but trigger p53 in human hematopoietic stem and progenitor cells. EMBO Mol Med 2017;9:1198–1211.
16. Szilvassy SJ, Meyerrose TE, Ragland PL, et al. Homing and engraftment defects in ex vivo expanded murine hematopoietic cells are associated with downregulation of β1 integrin. Exp Hematol 2001;29:1494–1502.
17. Zonari E, Desantis G, Petrillo C, et al. Efficient ex vivo engineering and expansion of highly purified human hematopoietic stem and progenitor cell populations for gene therapy. Stem Cell Reports 2017;8:977–990.
18. Radtke S, Humbert O, Kiem HP. Sorting out the best: Enriching hematopoietic stem cells for gene therapy and editing. Mol Ther 2018;26:2328–2329.
19. Baldwin K, Urbinati F, Romero Z, et al. Enrichment of human hematopoietic stem/progenitor cells facilitates transduction for stem cell gene therapy. Stem Cells 2015;33:1532–1542.
20. Masiuk KE, Brown D, Laborada J, et al. Improving gene therapy efficiency through the enrichment of human hematopoietic stem cells. Mol Ther 2017; 25:2163–2175.
21. Radtke S, Pande D, Cui M, et al. Purification of human CD34+CD90+ HSCs reduces target cell population and improves lentiviral transduction for gene therapy. Mol Ther Methods Clin Dev 2020; 18:679–691.
22. Araki H, Mahmud N, Milhem M, et al. Expansion of human umbilical cord blood SCID-repopulating cells using chromatin-modifying agents. Exp Hematol 2006;34:140–149.
23. Peled T, Shoham H, Aschengrau D, et al. Nicotinamide, a SIRT1 inhibitor, inhibits differentiation and facilitates expansion of hematopoietic progenitor cells with enhanced bone marrow homing and engraftment. Exp Hematol 2012;40:342–355.e1.
24. Heinz N, Ehrnström B, Schambach A, et al. Comparison of different cytokine conditions reveals resveratrol as a new molecule for ex vivo cultivation of cord blood-derived hematopoietic stem cells. Stem Cells Transl Med 2015;4:1064–1072.
25. Fares I, Chagraoui J, Gareau Y, et al. Pyrimidoindole derivatives are agonists of human hematopoietic stem cell self-renewal. Science 2014;345:1509–1512.
26. Cutler C, Multani P, Robbins D, et al. Prostaglandin-modulated Umbilical cord blood hematopoietic stem cell transplantation. Blood 2013;122:3074–3081.
27. Anjos-Afonso F, Currie E, Palmer HG, et al. CD34- cells at the apex of the human hematopoietic stem cell hierarchy have distinctive cellular and molecular signatures. Cell Stem Cell 2013;13:161–174.
28. Zou J, Zou P, Wang J, et al. Inhibition of p38 MAPK activity promotes ex vivo expansion of human cord blood hematopoietic stem cells. Ann Hematol 2012;91:813–823.
29. Gao Y, Yang P, Shen H, et al. Small-molecule inhibitors targeting INK4 protein p18 INK4C enhance ex vivo expansion of haematopoietic stem cells. Nat Commun 2015;6:1–10.
30. Guo B, Huang X, Cooper S, et al. Glucocorticoid hormone-induced chromatin remodeling enhances human hematopoietic stem cell homing and engraftment. Nat Med 2017;23:424–428.
31. Boitano AE, Wang J, Romeo R, et al. Aryl hydrocarbon receptor antagonists promote the expansion of human hematopoietic stem cells. Science 2010;329:1345–1348.
32. Xie SZ, Garcia-Prat L, Voisin V, et al. Sphingolipid modulation activates proteostasis programs to govern human hematopoietic stem cell self-renewal. Cell Stem Cell 2019;25:639–653.e7.
33. Notta F, Doulatov S, Laurenti E, et al. Isolation of single human hematopoietic stem cells capable of long-term multilineage engraftment. Science 2011;333:218–221.
34. Fares I, Chagraoui J, Lehnertz B, et al. EPCR expression marks UM171-expanded CD34+ cord blood stem cells. Blood 2017;129:3344–3351.
35. Radtke S, Görgens A, Kordelas L, et al. CD133 allows elaborated discrimination and quantification of haematopoietic progenitor subsets in human haematopoietic stem cell transplants. Br J Haematol 2015;169:868–878.
36. Subramaniam A, Talkhoncheh MS, Magnusson M, et al. Endothelial protein C receptor (EPCR) expression marks human fetal liver hematopoietic stem cells. Haematologica 2019;104:e47–e50.
37. Radtke S, Adair JE, Giese MA, et al. A distinct hematopoietic stem cell population for rapid multilineage engraftment in nonhuman primates. Sci Transl Med 2017;9:eaan1145.
38. Velten L, Haas SF, Raffel S, et al. Human haematopoietic stem cell lineage commitment is a continuous process. Nat Cell Biol 2017;19:271–281.
39. Tomellini E, Fares I, Lehnertz B, et al. Integrin-α3 is a functional marker of ex vivo expanded human long-term hematopoietic stem cells. Cell Rep 2019;28:1063–1073.e5.
40. Kirschner K, Chandra T, Kiselev V, et al. Proliferation drives aging-related functional decline in a subpopulation of the hematopoietic stem cell compartment. Cell Rep 2017;19:1503–1511.
41. Wang X, Dong F, Zhang S, et al. TGF-β1 negatively regulates the number and function of hematopoietic stem cells. Stem Cell Reports 2018; 11:274–287.
42. Cabezas-Wallscheid N, Buettner F, Sommerkamp P, et al. Vitamin A-retinoic acid signaling regulates hematopoietic stem cell dormancy. Cell 2017;169:807–823.e19.
43. Tolu SS, Wang K, Yan Z, et al. Characterization of hematopoiesis in sickle cell disease by prospective isolation of stem and progenitor cells. Cells 2020;9:2159.
44. Papa L, Zimran E, Djedaini M, et al. Ex vivo human HSC expansion requires coordination of cellular reprogramming with mitochondrial remodeling and p53 activation. Blood Adv 2018;2:2766–2779.
45. Lomova A, Clark DN, Campo-Fernandez B, et al. Improving gene editing outcomes in human hematopoietic stem and progenitor cells by temporal control of DNA repair. Stem Cells 2019;37:284–294.
46. Petrillo C, Thorne LG, Unali G, et al. Cyclosporine H overcomes innate immune restrictions to improve lentiviral transduction and gene editing in human hematopoietic stem cells. Cell Stem Cell 2018;23:820–832.e9.
47. Ferrari G, Thrasher AJ, Aiuti A. Gene therapy using haematopoietic stem and progenitor cells. Nat Rev Genet 2021;22:216–234.
48. Cavazzana M, Bushman FD, Miccio A, et al. Gene therapy targeting haematopoietic stem cells for inherited diseases: progress and challenges. Nat Rev Drug Discov 2019;18:447–462.
49. Scala S, Basso-Ricci L, Dionisio F, et al. Dynamics of genetically engineered hematopoietic stem and progenitor cells after autologous transplantation in humans. Nat Med 2018;24:1683–1690.
50. Six E, Guilloux A, Denis A, et al. Clonal tracking in gene therapy patients reveals a diversity of hu-

man hematopoietic differentiation programs. Blood 2020;135:1219–1231.

51. Larochelle A, Gillette JM, Desmond R, et al. Bone marrow homing and engraftment of human hematopoietic stem and progenitor cells is mediated by a polarized membrane domain. Blood 2012;119: 1848–1855.

52. Kallinikou K, Anjos-Afonso F, Blundell MP, et al. Engraftment defect of cytokine-cultured adult human mobilized CD34+ cells is related to reduced adhesion to bone marrow niche elements. Br J Haematol 2012;158:778–787.

53. J C, S G, JF S, et al. UM171 preserves epigenetic marks that are reduced in ex vivo culture of human HSCs via potentiation of the CLR3-KBTBD4 complex. Cell Stem Cell 2021;28:48–62.e6.

54. A S, K Ž, MS T, et al. Lysine-specific demethylase 1A restricts ex vivo propagation of human HSCs and is a target of UM171. Blood 2020;136:2151–2161.

55. Wagner JE, Brunstein CG, Boitano AE, et al. Phase I/II trial of StemRegenin-1 expanded umbilical cord blood hematopoietic stem cells supports testing as a stand-alone graft. Cell Stem Cell 2016;18:144–155.

56. Cohen S, Roy J, Lachance S, et al. Hematopoietic stem cell transplantation using single UM171-expanded cord blood: a single-arm, phase 1–2 safety and feasibility study. Lancet Haematol 2020;7:e134–e145.

57. Donahue RE, Jin P, Bonifacino AC, et al. Plerixafor (AMD3100) and granulocyte colony-stimulating factor (G-CSF) mobilize different CD34+ cell populations based on global gene and microRNA expression signatures. Blood 2009;114:2530–2541.

58. Teipel R, Oelschlägel U, Wetzko K, et al. Differences in cellular composition of peripheral blood stem cell grafts from healthy stem cell donors mobilized with either granulocyte colony-stimulating factor (G-CSF) alone or G-CSF and Plerixafor. Biol Blood Marrow Transplant 2018;24: 2171–2177.

59. Ozog S, Timberlake ND, Hermann K, et al. Resveratrol trimer enhances gene delivery to hematopoietic stem cells by reducing antiviral restriction at endosomes. Blood 2019;134:1298–1311.

60. Ngom M, Imren S, Maetzig T, et al. UM171 enhances lentiviral gene transfer and recovery of primitive human hematopoietic cells. Mol Ther Methods Clin Dev 2018;10:156–164.

61. Schiroli G, Conti A, Ferrari S, et al. Precise gene editing preserves hematopoietic stem cell function following transient p53-mediated DNA damage response. Cell Stem Cell 2019;24:551–565.e8.

62. Hu Y, Smyth GK. ELDA: extreme limiting dilution analysis for comparing depleted and enriched populations in stem cell and other assays. J Immunol Methods 2009;347:70–78.

Received for publication April 15, 2021;
accepted after revision August 19, 2021.

Published online: September 3, 2021.